

The Goblin Colony: Spectacular Monoliths and Walls of Altered Bandelier Tuff South of the Valles Caldera, New Mexico

Fraser Goff¹, Cathy J. Goff², Steve Chipera³, David Schiferl⁴, Laurie Waters⁵, Emiko Konishi⁶, Nels Iverson⁷, and Jean Gindreau⁸

¹ Department of Earth and Environmental Science, New Mexico Institute of Mining and Technology, Socorro, NM 87801, candf@swcp.com

² Independent Consultant, 5515 Quemazon, Los Alamos, NM 87544

³ Independent Consultant, 2408 Charleston Rd, Edmond, OK 73025

⁴ Pajarito Environmental Education Center, 2600 Canyon Rd, Los Alamos, NM 87544

⁵ Los Alamos National Laboratory (retired), Los Alamos, NM 87544

⁶ Chesapeake Energy Corporation, 6100 N. Western Ave, Oklahoma City, OK 73118

⁷ New Mexico Bureau of Geology and Mineral Resources, New Mexico Institute of Mining and Technology, 801 Leroy Pl, Socorro, NM 87801

⁸ PAC 8, 475 20th Street, Suite E, Los Alamos, NM 87544

Received November 2021, accepted March 2022. <https://doi.org/10.58799/NMG-v44n1.1>

Abstract

Detailed geologic mapping combined with petrologic and geochemical analyses and a low-altitude aerial drone survey were used to investigate the development of monoliths and walls of altered Bandelier Tuff at Goblin Colony (GC) 11 km south of the southern Valles Caldera rim in New Mexico. The monoliths and walls consist of eroded spires, fins, spire and fin clusters, columns, and steam pipes of bright orange to tan tuff. Mapping shows that nonwelded to poorly welded unit 1 (Qbt₁) of the Tshirege Member of the Bandelier Tuff (1.23 Ma) filled a preexisting southwest-trending canyon cut into a complex sequence of eroded Miocene volcanic lava flows, domes, dikes, and volcanoclastic debris flows and sandstones. A dacite dike and plug zone about 1.5 km long formed a hydrologic boundary on the southeastern margin of the canyon before tuff (ignimbrite) emplacement. Thin sections of altered tuff show growth of feathery and blocky zeolite minerals in glass shards, pumice, and pore spaces and on feldspar (sanidine) surfaces. Patches of secondary hematite-limonite are also common, resulting in the intense orange colors of tuff at GC. X-ray diffraction (XRD) analyses reveal that the zeolites are mordenite with lesser clinoptilolite, with the zeolites forming primarily at the expense of rhyolitic glass. Scanning electron microscope (SEM) images verify that zeolites are growing primarily on glass and in voids. XRD also reveals that the ignimbrite contains exceptionally low quantities of vapor-phase minerals, tridymite, cristobalite, and excess alkali feldspar, even if unaltered by zeolites. Whole-rock chemical analyses of altered tuff are not as revealing as other techniques but show relative increases in water, Al₂O₃, total Fe₂O₃, MgO, CaO, K₂O, and P₂O₅ and decreases in SiO₂ and Na₂O when compared with equivalent analyses of fresh tuff from the Pajarito Plateau. Concentrations of TiO₂ and MnO are unaffected.

An aerial drone survey was flown over GC to examine the orientation of structures. Vertical spires, fins, and clusters of zeolite-altered tuff are broadly aligned in a northeast–southwest pattern on the upper (north) part of GC. However, the drone survey revealed that most spires, fins, and clusters developed along elongate or curving cracks 10 to 50 m long in random orientations. Unaltered tuff surrounds the various features. Two imposing walls of zeolite-altered tuff also developed in a general northeast–southwest trend, but the north wall displays a pronounced southward undulation, and the south wall is cut by en echelon faults or fractures. Between the walls is a modern eroded ravine about 35 m deep. Columns and steam pipes of zeolite-altered tuff are found in the upper to middle portions of GC and plunge 70° to 60° northwest. The columns display considerable zeolite alteration, are best exposed in the uppermost north part of GC, and are surrounded by unaltered tuff. Steam pipes protrude from the south face of the north wall; their rinds are zeolite-rich and their cores contain minor amounts of mordenite. The bottom of the GC sequence reveals a broad area of "tables" that display horizontal ledges of zeolite-altered tuff, and that can be traced for nearly a kilometer upstream of the main GC sequence.

We compared low-temperature (zeolite-producing) hydrothermal processes at GC to other gas-release phenomena in ignimbrites, including some that occur elsewhere in the Bandelier Tuff. Our interpretation of the mapping and other data at GC is that the Tshirege ignimbrite that filled the paleocanyon there was cooled and probably gas-depleted due to distal flow over rugged topography. It was emplaced at temperatures ≤400°C, well below temperatures associated with typical vapor-phase alteration (tridymite, cristobalite, and alkali feldspar assemblages). Tshirege ignimbrite interacted with cold surface water or saturated ground (small pond, marsh, or cold springs) in the canyon bottom. Hydrothermal fluids that rose toward the top of the tuff sequence in fumaroles created nearly vertical structures, including columns, pipes, spires, and other features. The fluids were moderately alkaline and formed zeolites (mordenite and clinoptilolite) by reacting with glass, achieving temperatures as high as 200°C at the upper stability limit of mordenite in most hydrothermal systems. As fumarolic activity waned, internal compaction, slumping (?), and fracturing of tuff along with simultaneous hydrothermal fluid circulation formed walls and other features. Based on analogies with the Valley of Ten Thousand Smokes (VTTS) ignimbrite (Alaska), the entire hydrothermal event at GC probably lasted no more than 100 to 200 years. Because altered tuff is more resistant to weathering than non-welded tuff, GC preserves a 100-m-high slope of intricate monoliths and imposing walls along a post-tuff drainage (a tributary of Paliza Canyon) that has cut a notch through the Miocene dike zone.

Introduction

Goblin Colony (GC) is an area of stunningly beautiful, altered Bandelier Tuff located in the southern Jemez Mountains about 11 km south of the southern Valles Caldera rim and about 5 km north of the village of Ponderosa (Fig. 1). The name is thought to derive from the sound of wind blowing through features that look like goblin faces on moonlit nights (see cover photo). Goblin Colony consists of about 0.15 km² (37 acres) of pronounced vertical spires, fins, spire and fin clusters, walls, columns, and tabular ledges that occupy a steep, south-facing slope on the north side of a tributary of Paliza Canyon (informally called Goblin creek on Fig. 2). Goblin Colony also resides in a broader region of canyons, arroyos, and cliffs that expose older, eroded volcanic rocks and sediments of the Jemez Mountains volcanic field (JMVF). Because of the statuesque nature of the goblins, some of which look eerily like eroded faces, this area has become a destination for hikers who want an easy but rewarding adventure (Holsapple, 2019, 2021). However, these websites provide no geologic explanation for how GC and the surrounding rocks were formed. Thus, the authors spent several months in summer 2021 compiling a detailed geologic map of the area and determining petrographic and geochemical characteristics of the rocks. We combined these data with a low-altitude aerial drone survey to determine how GC formed.

Goblin Colony Geology

Goblin Colony is located south of the Valles Caldera within the canyon country of the southern Jemez Mountains (Figs. 1 and 2) where older volcanic rocks of the JMVF overlie early basin-fill sediments of the Rio Grande rift and Mesozoic/Paleozoic strata on the east-tilted dip slope of the Sierra Nacimiento Laramide highland (see geologic maps of Smith et al., 1970; Gardner, 1985; Osburn et al., 2002; Kempter et al., 2007). The southern JMVF consists of basaltic through rhyolitic rocks and associated sediments of the Keres Group (primarily the Paliza Canyon Formation [PCF]) overlain by pyroclastic flow and fall deposits of the Tewa Group (the Bandelier Tuff; see Gardner et al., 2010; Goff et al., 2011; and Kelley et al., 2013b for the latest stratigraphic nomenclature in the JMVF). The above authors did not discuss the unusual rock features composed of the Tshirege Member of the Bandelier Tuff that make up GC. However, two field trip guidebooks through the southern Jemez Mountains have mentioned vapor-phase pipes in the Tshirege Member that are exposed along Forest Service Road 10 (FS10) north of Ponderosa (Fig. 1). Self et al. (1996, p. 34) and Kelley et al. (2007, p. 120) also noted these features. These pipes (columns) are exposed along a roadcut on the extreme northwestern margin of GC (Figs. 2 and 3).

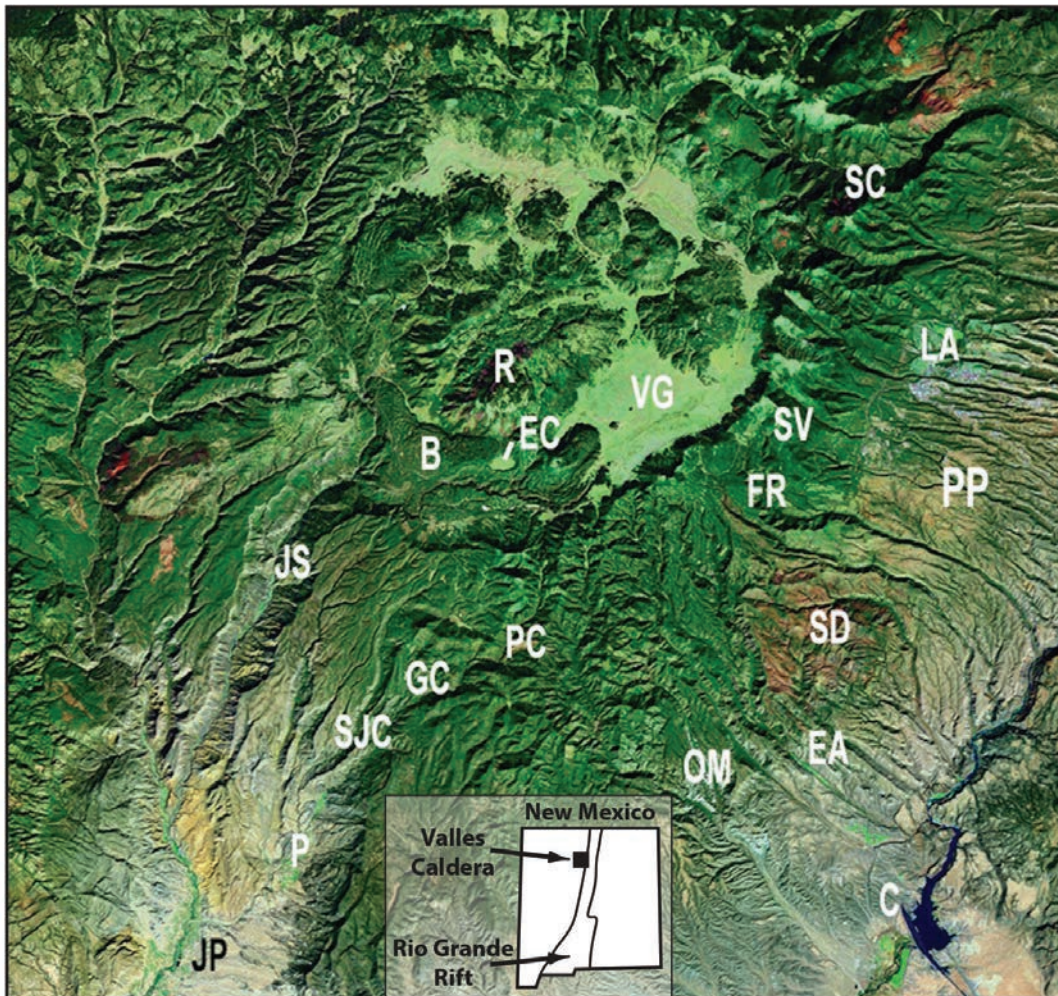
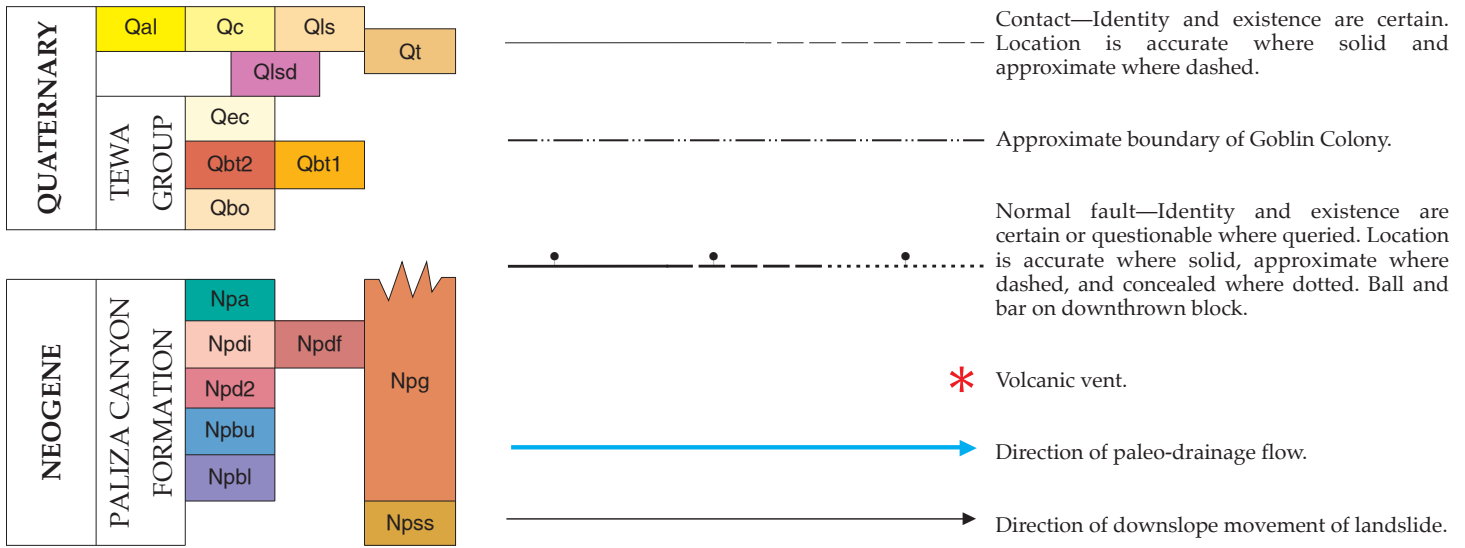


Figure 1. Color-enhanced LANDSAT photo shows the Valles Caldera (1.23 Ma; Phillips et al., 2007; Nasholds and Zimmerer, 2022) and southern Jemez Mountains region, New Mexico. The caldera is approximately 22 km in diameter; north is at top of image. Goblin Colony (GC) is located about 11 km south of the southern edge of Valles Caldera on an unnamed creek (Paliza Canyon tributary) roughly 0.5 km north of Paliza Canyon (PC).

Labels:

- B = Banco Bonito lava flow, youngest eruption in Valles Caldera (68 ka; Zimmerer et al., 2016)
- C = Cochiti dam and reservoir on the Rio Grande
- EA = Eagle Canyon
- EC = El Cajete crater
- FR = upper Frijoles Canyon
- GC = Goblin Colony
- JP = Jemez Pueblo on the Rio Jemez
- JS = town of Jemez Springs
- LA = city of Los Alamos
- OM = Oaks Mesa
- P = village of Ponderosa
- PC = Paliza Canyon
- PP = Pajarito Plateau
- R = Redondo Peak, highest point on the Valles resurgent dome (3,430 m)
- SC = Santa Clara Canyon
- SD = St. Peter's Dome
- SJC = San Juan Canyon
- SV = Sierra de los Valles
- VG = Valle Grande



QUATERNARY

HOLOCENE

- Qal** Valley Bottom Alluvium—Valley bottom alluvium; may contain some terrace gravel along lower Paliza Canyon.
- Qc** Colluvium, Talus, and Slope Wash—Colluvium, talus, and slope wash.
- Qls** Landslide Deposits—Landslide deposits.
- Qt** Terrace Deposits—Terrace deposits consisting of sand, gravel and silt that underlie young terrace surfaces bordering present streams.
- Qlzd** Dacite Landslide Deposits—Dacite landslide deposits.

TEWA GROUP

- Qec** El Cajete Pyroclastic Beds—Locally the beds are extremely thick or thin depending on mass wasting. Dated at an age of 74.7 ± 1.3 ka (Zimmerer et al., 2016).
- Qbt2** Tshirege Member of the Bandelier Tuff, flow unit 2—Non-welded to poorly welded rhyolitic ignimbrite with obvious chatoyant sandine; forms uniform sheet ± 10 m thick in west and north parts of map; base of unit contains discontinuous surge deposits.
- Qbt1** Tshirege Member of the Bandelier Tuff, flow unit 1—Non-welded to poorly welded rhyolitic ignimbrite with variable alteration; thickness is 5–98 m depending on location; contains ± 40 cm of basal Tsankawi Pumice at several locations in map area. Dated at an age of 1.231 ± 0.001 Ma (Phillips et al., 2007; Nasholds and Zimmerer, 2022).
- Qbo** Otowi Member of the Bandelier Tuff—Non-welded to poorly welded, lithic-rich, rhyolitic ignimbrite; thickness = 30 m. Dated at an age of 1.61 ± 0.01 Ma (Izett and Obradovich, 1994).

NEOGENE

PALIZA CANYON FORMATION

- Npg** Gravel, Conglomerate, Debris Flows—Volcaniclastic gravel, conglomerate, debris flows, hyper-concentrated flows, and minor fluvial sandstone of the Paliza Canyon Formation; interlayered with Paliza Canyon volcanic rocks; thickness ≤ 85 m.
- Npa** Andesite Plug—Dark gray eroded plug (and flow?) of fine-grained, two-pyroxene andesite, Paliza Canyon Formation.
- Npdi** Dacite Intrusions—Tan to gray biotite dacite intrusions forming two circular plugs and an elongate dike; much of the dike is partially hidden by El Cajete Pyroclastic Beds.
- Npdf** Dacite Flows—Gray biotite dacite lava flow originating from the plugs mentioned previously; southwest flow contains horizontal columnar joints; thickness of flows ≤ 15 m.
- Npd2** Dacite Plug—Dark gray to black, aphyric, biotite-hornblende dacite plug; extreme near-vertical sheeting on southeast side.
- Npbu** Upper Basalt—Dark gray olivine basalt, upper flow; mostly 3–5 m thick; interlayered in unit Npg. Dated at an age of 9.45 ± 0.07 Ma (Goff et al., 2006).
- Npbl** Lower Basalt—Dark gray olivine basalt, lower flow 5–10 m thick; underlies Npg; overlies Npss in lower Paliza Canyon. Dated at an age of 9.54 ± 0.08 Ma (Kempster et al., 2007).
- Npss** Sandstone and Conglomerate—Tan, bedded to cross-bedded volcanic sandstone and minor thin beds of matrix-supported volcanic conglomerate; contains some white clasts of altered pumice (Canovas Canyon tuffs?), but most clasts are rhyolite and basalt; thickness about 10–15 m.

Paliza Canyon Formation, Keres Group

We prepared a detailed geologic map of the GC area using a portion of the Bear Springs Peak quadrangle map of Kempton et al. (2007) as our base (Fig. 2). Our mapping and other studies were supported with 11 thin sections and several chemical analyses (Supplemental Data [SD] 1)¹. Paliza Canyon Formation volcanic and volcanoclastic rocks make up the majority of map units in the GC area and are part of the Keres Group. The Keres Group contains all volcanic units erupted in the JMVf prior to the formation of the Valles and Toledo calderas and the Bandelier Tuff (which is part of the overlying Tewa Group; Gardner et al., 2010; Goff et al., 2011; Kelley et al., 2013b).

Volcaniclastic Deposits, Npss and Npg: Volcaniclastic deposits make up a significant portion of the PCF due to erosion of contemporaneous tuffs, lava flows, and lava domes. These deposits thicken to the south, southeast, and southwest. They are the oldest rocks within the immediate area of GC. Unit Npss consists of fluvial sandstone and thin, interbedded, matrix-supported conglomerate (Figs. 4a and 4b), and may be equivalent to some sandstone units mapped as part of the Canovas Canyon Formation (e.g., Kempton et al., 2007). However, unit Npss is lumped within generic volcanoclastic deposits (Tpv) on the map of Kempton et al. (2007). Unit Npss underlies an approximately 10-m-thick flow of olivine basalt (aka the lower basalt, Npbl) along lower Paliza Canyon, is cut by a prominent dacite dike (Npdi) and other intrusions in the Paliza Canyon tributary, and extends roughly 0.5 km upstream along the creek. Where clearly observable, unit Npss is about 15 m thick. The sandstone apparently underlies the southern part of the Tshirege Member at GC. The sandstone is fine to medium grained and contains primarily quartz, feldspar, and a few tiny lithics. Much of the feldspar is slightly pink, indicating it is probably microcline. This sand resembles much of the sand in the Abiquiu Formation that crops out about 4 km north of GC (Goff et al., 2006). The conglomerate within Npss contains a variety of volcanic clasts, but white pumice and gray rhyolite (possibly from the Canovas Canyon Formation, erupted about 9.75 to 8.8 Ma) and sparse basalt are most obvious (Kempton et al., 2007).

Unit Npg (Fig. 2; mostly equivalent to Tpv in Kempton et al., 2007) consists primarily of interlayered gravel, conglomerate, debris flows, and hyperconcentrated-flow deposits (Fig. 5). Fluvial sandstone is a minor component. Some of the boulders are larger than an automobile, but most are ≤ 0.5 m. Most clasts consist of basalt, andesite, or dacite. Rhyolite is subordinate. Within our map area, the best exposures of Npg occur east of the Paliza Canyon tributary along the steep walls of Paliza Canyon where it is ≤ 85 m thick. Npg overlies the lower basalt (Npbl), but it is interlayered with the upper olivine basalt (Npbu) and other lava flows.

Olivine Basalt: Two lava flows of olivine basalt, each roughly 10 m thick, are interlayered with volcanoclastic rocks along Paliza Canyon (SD1; Fig. 4a). Both consist of porphyritic volcanic rock



Figure 3. Outcrop of vapor phase pipes along FS10 below Goblin Mesa first described by Self et al. (1996); the pipes appear as columns of harder material cemented by zeolite minerals mordenite and clinoptilolite. The columns are inclined to the southwest. Softer ignimbrite material between the columns is virtually devoid of zeolites.



Figure 4. Photos of volcanoclastic deposits of the Keres Group, map unit Npss. **a)** Mixed sandstone and conglomerate beds underlying the lower olivine basalt (upper left; Npbl) along lower northwest wall of Paliza Canyon (Fig. 2). Beds dip slightly to southwest. **b)** Close-up photo of Npss. Note white pumice probably from eroded tuffs in the Canovas Canyon Formation. Hammer handle for scale.

¹ Supplemental Data tables are available at <https://geoinfo.nmt.edu/repository/index.cfm?rid=20230001>

with phenocrysts of plagioclase, clinopyroxene, and olivine in a dark gray, fine-grained matrix of the same three minerals plus opaque oxides and minor glass. Olivine in the lower basalt (Npbl) is pervasively altered to reddish-orange high-temperature iddingsite (an intimate mixture of orthopyroxene, maghemite, hematite, cristobalite, and amorphous silica; Goff, 1996, p. 173). Unit Npbl is dated at 9.54 ± 0.08 Ma at a location east of our map (Kempster et al., 2007). Texture and mineralogy in the upper flow (Npbu) are similar to the lower flow that shows some high-temperature iddingsite alteration as described above. Unit Npbu is not dated in our map area but may be equivalent to a similar lava flow 4 km to the north dated at 9.45 ± 0.07 Ma (Goff et al., 2006).

Dacite to Andesite Intrusions and Flows: The youngest PCF volcanic units on the map consist of a northeast-trending group of dacite to andesite intrusions and lava flows expressed mostly as plugs and dikes. The most extensive unit of this group is a fine-grained gray to tan dacite (SD1; unit Npdi) with very sparse phenocrysts of small biotite and plagioclase. The matrix consists of microphenocrysts of felty plagioclase surrounded by devitrified glass, smudgy opaque oxides, and 10% small vesicles. Unit Npdi forms two tall plugs and a long dike that crosses the tributary of Paliza Canyon and extends northeast along the drainage for another 0.5 km (Figs. 2, 6, and 7). The dike is partly buried by pumice from El Cajete crater (Fig. 2); thus, its extent was not previously appreciated. The two plugs are separated from each other by a stack of interlayered lava flows and volcanoclastic rocks (Npbl, Npg, and Npdf). Given their identical appearance, a deeply buried dacite dike probably connects the two plugs. The uppermost lava flow in the aforementioned stack (Npdf) consists of the same type of dacite as the plugs and dike. The southwestern exposure of the flow underlies Bandelier Tuff and displays horizontal columnar joints, indicating that it filled and solidified against a previous valley wall.

The northeastern dacite plug is intruded and overlain by dark gray, fine-grained andesite (Npa) that contains sparse small phenocrysts of plagioclase in a groundmass of plagioclase microlites, small ortho- and clinopyroxene crystals, and black opaque-oxide-rich glass. We could find no associated lava flow for this andesite intrusion, but it clearly overlies the dacite plug (Npdi).

A third volcanic plug (Npd2) forms a small northeast-elongated hill just southeast of the previously mentioned dacite plug and dike zone (Fig. 2; see Gardner, 1985). The plug consists of dark gray to black, nearly aphyric dacite (SD1) with very sparse phenocrysts of biotite, hornblende, and plagioclase. On the east side of the intrusion where it is exposed by erosion along Paliza Canyon, Npd2 displays nearly vertical foliation. Large vesicles on the northwestern side of the Npd2 vent are partially filled with vapor-phase quartz.

The above three intrusive units and lava flows are not dated, but Gardner (1985, p. 36) indicated they were probably emplaced 9 to 7 Ma. Additionally, all three of the intrusive units have baked volcanoclastic rocks along their margins (e.g., Npss) where these relations can be observed.



Figure 5. Photo of volcanic debris flows in Npg, on southeast wall of Paliza Canyon about 30 m above canyon floor. Grass and small shrubs for scale.



Figure 6. Photo looking northwest of dacite dike (Npdi) where it is crossed by the Paliza Canyon tributary and an abandoned forest service road. The southwest (left) part of the dike rises abruptly to form a plug a few hundred meters above the valley floor.

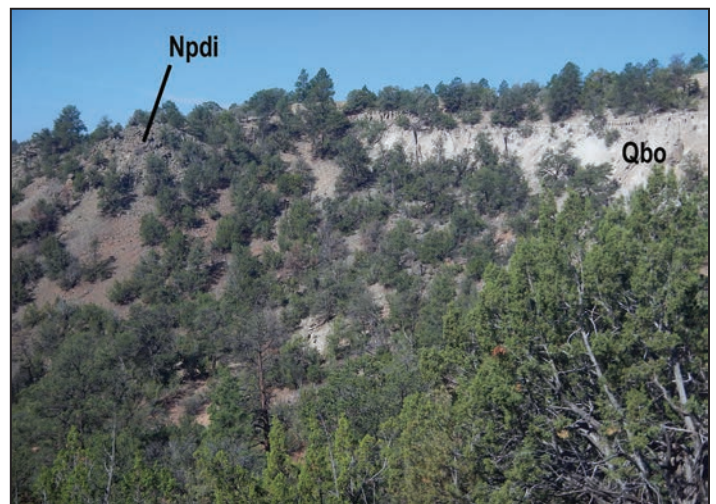


Figure 7. Photo looking west at Otowi Member (Qbo) abutting the north side of the southwestern dacite plug (Npdi). At this location, Qbo is overlain by a thin layer of Tshirege Member (Qbt). Npdi intrudes Paliza Canyon gravels (Npg) along a vertical contact on its southwestern side.

Tewa Group

Otowi Member of the Bandelier Tuff: The Otowi Member of the Bandelier Tuff (Qbo; Fig. 2) erupted during formation of the Toledo Caldera at 1.61 ± 0.01 Ma (Izett and Obradovich, 1994; Gardner et al., 2010; Goff et al., 2011; Kelley et al., 2013b). The Otowi Member consists of white, nonwelded to poorly welded ignimbrite containing white pumice and $\geq 2\%$ conspicuous dark lithic clasts, mostly PCF volcanic rocks. Quartz and sanidine phenocrysts make up about 5% to 10% of the bulk rock. Unit Qbo is best exposed in the southwestern part of our geologic map (Fig. 2) where it fills a previously unrecognized small valley and underlies the Tsankawi Pumice and Tshirege Member. The Otowi Member also abuts against the earlier volcanic plug of dacite mentioned previously (Npdi; Fig. 7).

Tshirege Member of the Bandelier Tuff: The Tshirege Member of the Bandelier Tuff (Qbt; Fig. 2) erupted from the Valles Caldera at 1.231 ± 0.001 Ma (Smith and Bailey, 1968; Phillips et al., 2007; Goff, 2009, 2010; Kelley et al., 2013b; Nasholds and Zimmerer, 2022). The Tshirege Member is perhaps the most impressive volcanic deposit in the Jemez Mountains because of its distinct color (tanish and pinkish orange), widespread distribution, large volume (roughly 400 km^3), thickness (often >50 m), cliff-forming nature, and propensity to fill preexisting canyons such as those in Bandelier National Monument. The Tshirege Member consists of a series of rhyolitic ash-flow (ignimbrite) sheets and tongues that spread out in all directions during caldera formation (Smith and Bailey, 1966; Smith et al., 1970; Goff et al., 2011, 2014, fig. 3).

Within our map area, the Tshirege consists of the two lowest flow units that are recognizable around the caldera (Sussman et al., 2011; see Goff et al., 2014, fig. 3 for the most recent and complete Tshirege flow-unit stratigraphy). Tshirege unit 1 (Qbt₁) is the first ignimbrite package erupted from Valles Caldera and is the most voluminous and extensive (Broxton and Reneau, 1995; Goff et al., 2014, fig. 3, table 1). The spires, walls, tabular ledges, and other landforms of GC (Figs. 8a–f) have formed entirely within unit Qbt₁. The thickness of Qbt₁ at GC is about 95 m, but elsewhere in the area it is usually <50 m. Unit Qbt₁ consists of bright orange to gray, altered, nonwelded to poorly welded (sintered), porphyritic ignimbrite. The tuff contains about 10–20% crystals of quartz and sanidine, and trace amounts of mafic minerals in a low-density matrix of vesiculated ash and pumice. The pumice is light colored and typically contains $\leq 5\%$ phenocrysts. Lithic content is $\leq 1\%$ of the total bulk rock. Average lithic size varies from ≤ 5 cm near the top of Qbt₁ to ≤ 3 cm near the middle. Most lithics consist of dark-colored precaldera volcanics, mostly basalt, andesite, and dacite.

Unit Qbt₁ also contains $<1\%$ of light-colored hornblende dacite pumice (Bailey et al., 1969; Stimac, 1996; Goff et al., 2014; Boro et al., 2020). Hornblende dacite pumice fragments are low density and vesicular, are generally ≤ 10 cm long, and contain small phenocrysts of hornblende, plagioclase, biotite, and minor pyroxene. In our work at GC, hornblende dacite pumice was smaller and more difficult to find at the top of Qbt₁ than in the middle of the unit, where we found several specimens in about 30 minutes.

Unit Qbt₁ at GC is underlain by roughly 40 to 60 cm of the Tsankawi Pumice Bed, the pyroclastic fall deposit representing the initial eruption of the Tshirege Member (Fig. 9; Bailey et al., 1969; Gardner et al., 1986, 2010; Goff et al., 2014). White Tsankawi Pumice deposits can be traced sporadically upstream over a distance of several hundred meters along the northern side of the Paliza Canyon tributary. A poorly exposed soil developed on top of the PCF and is preserved beneath the Tsankawi Pumice Bed in this area.

Unit 2 of the Tshirege Member (Qbt₂) forms a ledge about 10 m thick (Fig. 10) that overlies Qbt₁ in the map area. Unit Qbt₂ is separated from Qbt₁ by a discontinuous layer of pyroclastic surge deposits ≤ 0.5 m thick. Unit 2 is eroded away at the top of GC along FS10 (Fig. 2), possibly due to alteration. All that is left of Qbt₂ there is a lag of nonwelded to poorly welded Qbt₂ blocks and fragments that contribute to colluvial deposits downslope (e.g., the fan deposit in Fig. 8a). Otherwise, Qbt₂ consists of pale tan to gray, poorly to moderately welded, porphyritic ignimbrite that is generally harder and denser than Qbt₁. Because of welding and compaction, phenocrysts of quartz and feldspar seemingly make up roughly 30% of Qbt₂ and the lithic content is $\leq 1\%$. Sanidine phenocrysts in Qbt₂ are cryptoperthitic (Keefer and Brown, 1978) and display striking peacock blue iridescence (adularescence or chatoyancy; Deer et al., 1992, p. 393 and p. 406; Smith and Brown, 1988, chapter 19 and fig. 19.9) caused by unmixing of albite from original sanidine during rapid cooling of the ignimbrite. Iridescent sanidine is less conspicuous in Qbt₁ within GC, but is better displayed elsewhere in the Jemez Mountains.

El Cajete Pyroclastic Beds: The youngest volcanic rock unit in the map area (Fig. 2) consists of a discontinuous blanket of El Cajete Pyroclastic Beds white fall deposits (74.4 ± 1.3 ka; Gardner et al., 2010; Kelley et al., 2013b; Zimmerer et al., 2016). Within the map area, these pumice deposits were previously mined over a period of more than 50 years. El Cajete deposits (Qec) originated from a crater along the southern part of the Valles Caldera ring fracture zone (Fig. 1). The pumice is very low density and contains small phenocrysts of quartz, feldspar, and biotite and small amounts of other mafic minerals. El Cajete pumice is distinguished from Bandelier Tuff pumice by the presence of obvious biotite. El Cajete pumice caps mesa tops (Fig. 10) and has been eroded into south- to east-facing swales, gullies, and valleys covering critical contacts and other rock units. Thickness of the El Cajete is generally ≤ 20 m.

Large-Scale Structures

Faults: We could not identify any faults within GC proper except possibly at the northeastern end of south wall (see below). However, we found one probable north-trending fault in the southwestern part of the map area (Fig. 2), which apparently offsets the Tshirege Member by 1 or 2 m, down to the west. The faulted area of Tshirege contains north-trending fractures. The fault was probably active before eruption of the Tshirege Member because it appears to uplift the dacite lava flow (Npdf) and underlying Paliza Canyon gravels (Npg) against the

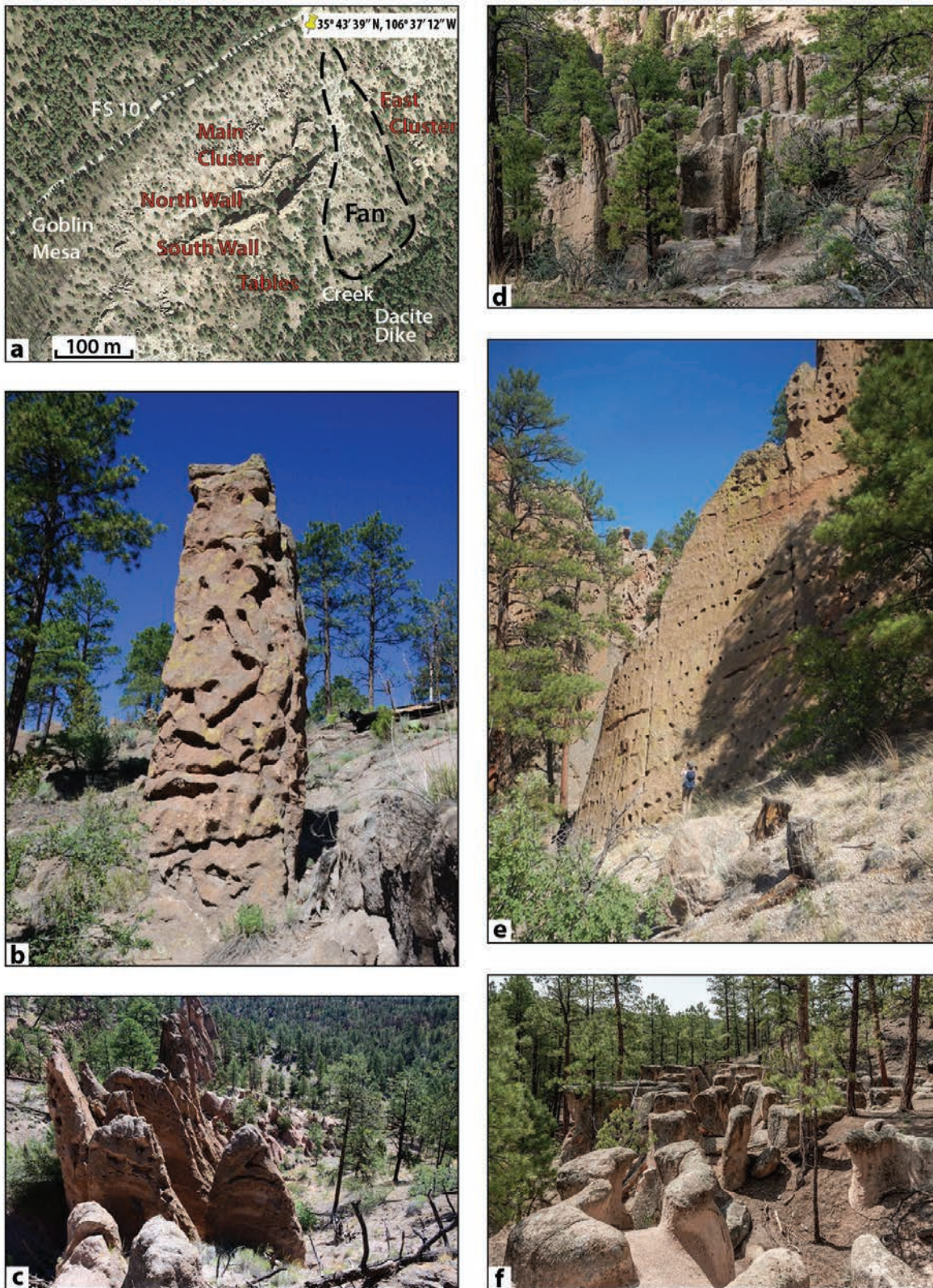


Figure 8. Images of GC features. **a)** Cropped and labeled Google Maps image of GC located southeast of FS10 at UTM NAD27 353536E, 3954731N. Goblin Colony features consist of three regimes: the southwest-trending main cluster of spires, a pair of southwest to west-southwest-trending north and south walls, and an area of exposed tabular ledges near the point where ravines eroding the slopes of the features enter the Paliza Canyon tributary. A fan composed of colluvium of Tshirege units overlain by El Cajete pumice deposits divides the features described above from the east cluster of spires. Note the deep ravine that separates the north and south walls (black due to shade). **b)** A single spire or goblin in the main cluster (Fig. 8a). The upper part of the spire looks like a face or head. **c)** A phalanx of goblins standing sentinel in main cluster, view looking northeast. Lines of goblins are reminiscent of the famous Moai statues at Rapa Nui (Easter Island) in the southern Pacific Ocean. Although they appear as a line, the goblins are commonly clustered. **d)** Looking southwest toward the main cluster of goblins. **e)** South face of the south wall, looking north; human for scale at bottom of cliff. Note the subparallel lines of erosion cavities that mimic the slope of the land surface. These lines of erosion cavities are present in all types of features at GC (see base of spire, Fig. 8b) and in the Bandelier Tuff throughout the Jemez Mountains. **f)** In the tabular ledges area, looking south toward the Paliza Canyon tributary.

Otowi Member (Qbo). The fault is not easily traceable to the south or north because it is hidden in colluvium and El Cajete deposits, respectively.

A north-trending fault just beyond the northeastern part of the map area was identified by Kempter et al. (2007). It displaces the Tshirege Member and the offset is about 20 m down to the east. Two north-trending faults were identified by Goff et al. (2006) in the southern part of the Redondo Peak quadrangle 4 to 6 km north of GC. These faults cut the Tshirege Member and older rock units, including the Abiquiu Formation (with an age of approximately 25 to 19 Ma; Osburn et al., 2002; Kelley et al., 2013a).

Dike and Intrusion Zone: The dacite plugs and dike (Npdi) were injected into older PCF units at 9 to 7 Ma along an obvious north-northeast-trending fault or fracture zone (Fig. 2), but offset along this structure is not obvious. In a broader context, the andesite (Npa) and the other dacite intrusion (Npd2) probably erupted along this same zone. All of these faults, fractures, and intrusions are part of the north-trending Cañada del Cochiti fault zone originally defined by Gardner (1985; see also Kelley et al., 2013b). The stress regime of this zone is related to evolution of the Rio Grande rift, and faulting consists mostly of progressive north-trending and northeast-trending structures through time (Kelley et al., 2013b).

Paleo Geomorphology and Stream Drainages: The southern Jemez Mountains presently contain many impressive canyons such as San Juan and Paliza canyons, but our mapping and other observations indicate that at least two paleovalleys, basins, or drainages were filled and abolished. The first is the probable valley in the southwestern part of our map area that was filled with Otowi Member (Figs. 2 and 7). In this area, the Otowi Member overlies PCF gravels (Npg), is overlain by the Tshirege Member (Qbt₁ and Qbt₂), and is not traceable to the north except for a poor exposure facing San Juan Canyon in the northwestern corner of the map area.

The second eradicated drainage is younger. This drainage was excavated on the northwestern side of the northeast-trending dike and plug complex described above (Fig. 2). The intrusive bodies (Npdi, etc.) created an impermeable or restrictive barrier to erosion and surface-water flow to the south. The paleodrainage formed after eruption of the Otowi Member when a stream cut deeply into a preexisting layered sequence of Otowi ignimbrite and PCF lava flows and volcaniclastic rocks, of which only remnants presently exist. This drainage had a southwesterly flow direction, semiparallel to the dacite plug and dike complex, but was later filled with ignimbrites of the Tshirege Member. Goblin Colony rock formations that developed in the Tshirege Member presumably formed above sedimentary deposits that accumulated in this younger drainage, which may have included water-saturated pond or marsh deposits.

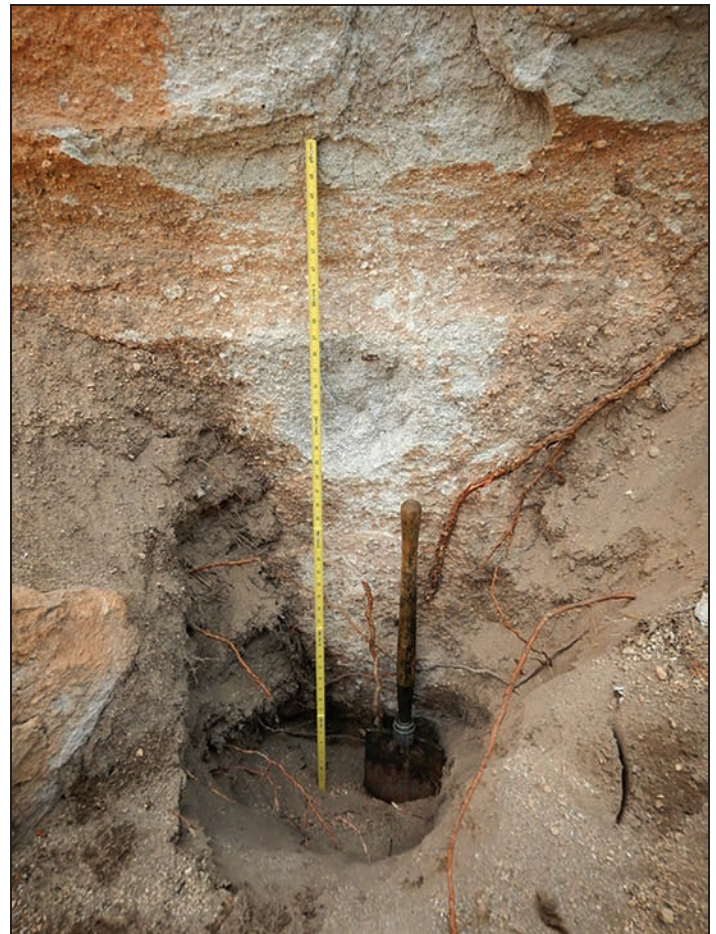


Figure 9. Pit dug into the base of the Tsankawi Pumice in the tabular ledges area of GC (Fig. 8a). The Tsankawi rests on a soil developed at the top of Paliza Canyon volcaniclastic unit Npss (Fig. 2). Within the soil are abundant small gravel fragments of Paliza Canyon volcanics.

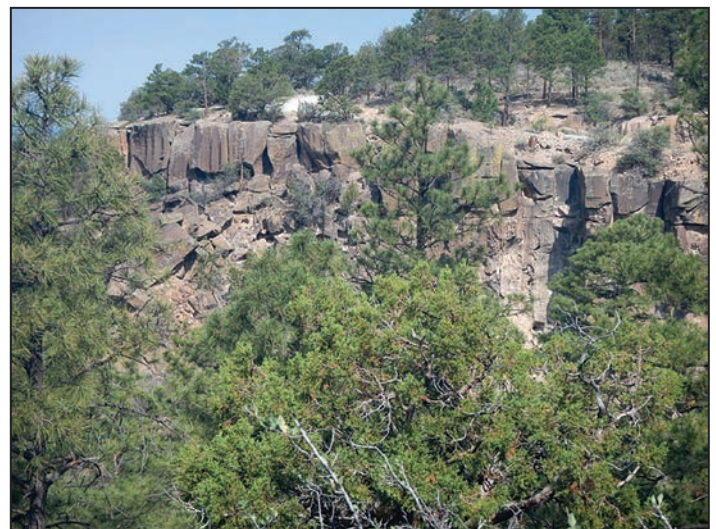


Figure 10. Unit Qbt₂ of the Tshirege Member forms a ledge of partly to densely welded ignimbrite overlying unit Qbt₁. Forest Service Road 10 is visible on top of the ledge. Above Qbt₂ is a rounded thick deposit of El Cajete Pyroclastic Beds (Qec, Fig. 2) that have been intermittently mined for decades.

Analytical Methods

We obtained 11 standard thin sections, six of PCF volcanics from the broader map area and five of Tshirege Member at GC proper (SD1 and SD2). The first six sections were used to identify and verify rock names and phenocryst assemblages in the older volcanic flows and intrusions of the map area (Fig. 2; see above). The five Qbt₁ sections were used to determine textures, phenocryst assemblages, and alteration mineralogy in GC rocks, and to compare with XRD results from other Tshirege Member samples (described below).

XRD analyses were performed on eight samples (SD3) at the Reservoir Technology Center Lab, Chesapeake Energy Corporation. Samples were first powdered by hand with an alumina mortar and pestle. A small portion of each sample (approximately 1.6 g) was mixed with 1.0 µm corundum (Al₂O₃) internal standard in the ratio 80% sample to 20% corundum by weight. Each sample was then ground under acetone in a McCrone micronizing mill (fitted with an agate grinding set) for 10 minutes. All diffraction patterns were collected on a Bruker D8 X-ray powder diffractometer using CuKα radiation and a LYNXEYE position sensitive detector, from 2° to 70° 2θ using approximately 0.04° steps.

Mineral abundances were determined using FULLPAT, a quantitative X-ray powder diffraction (QXRD) program and method, originally developed in the Earth and Environmental Sciences Division at Los Alamos National Laboratory (Chiperia and Bish, 2002, 2013). FULLPAT matches entire patterns including the background and utilizes a least-squares refinement to optimize the fitting of the library standards to the observed pattern. The advantage of FULLPAT over other QXRD methods is that amorphous components are explicitly analyzed by fitting the entire background, rather than estimating the abundance of amorphous phases as 100% minus the sum of crystalline phases.

Scanning electron microscope (SEM) images were obtained on a Hitachi S-4800 Field Emission SEM instrument at the New Mexico Bureau of Geology and Mineral Resources. Dust and fine grit from altered patches of seven Qbt₁ samples listed in SD3 were mounted on SEM stubs with double-sided carbon tape and platinum coated. All images were taken with a 5 or 10 kV accelerating voltage and 10 µA beam current. Lower accelerating voltages were needed to produce images of delicate zeolite crystals that highlight various alteration textures.

Whole-rock major and trace element chemical analyses of five unaltered and altered Qbt₁ samples (SD3) were obtained from ALS Global, Reno, Nevada, using their complete characterization package that combines X-ray fluorescence (XRF) and inductively coupled plasma mass spectrometry (ICP-MS) methods (ALS Global, 2021, p. 35). These analyses were used to look for added water or other volatile components and to determine if specific elements were added or leached because of hydrothermal alteration. We also obtained a single analysis of a dike from unit Npdi because it had not been previously analyzed. Results (SD1 and SD2) are compared with previously published analyses of PCF units and fresh Tshirege units Qbt₁ and Qbt₂.

Results

Thin Sections: Five thin sections were prepared of Tshirege Member samples at GC, one of relatively fresh tuff and four of altered tuff. A sample of fresh, nonwelded Tshirege unit 2 (Qbt₂; Fig. 11a), from a location that is a meter above the basal contact with the underlying Qbt₁, shows eutaxitic texture and consists of approximately 50% voids including vesicles, 30% pale brown glass shards, 15% phenocrysts of sanidine and quartz, 4% pumice, 1% lithic fragments, and <1% opaque oxides (total = 100%). There were also three crystals of Fe-rich augite, one crystal of fayalite (a trace component of lower Tshirege ignimbrites; Warshaw and Smith, 1988; Goff et al., 2014), three small clasts of hornblende dacite pumice, and perhaps five crystals of plagioclase, although the latter may be from disaggregated lithic fragments. Some of the larger lithic fragments contain small plagioclase and are volcanic in origin. There were no primary plagioclase crystals with distinctive albite twinning. A large proportion of the phenocrysts are broken crystals typical of explosive pyroclastic deposits. Larger quartz crystals are often embayed, and a few are euhedral. Sanidine crystals are typically blocky, and some show cleavage or partings and a few show Carlsbad twinning. The glass is fresh and devitrification is minor to absent.

In contrast, four thin sections of Tshirege unit 1 (Qbt₁) from GC show obvious eutaxitic texture, but also show variable amounts of altered glass. Most of the alteration probably formed zeolite minerals (Fig. 11b), although some of the alteration may be minor devitrification; thus, there are somewhat fewer voids. Overall, there appear to be slightly more lithics and pumice, but about the same amount of phenocrysts as in Qbt₂. The primary phenocryst minerals are quartz and sanidine. Both appear to be fresh. Some sanidine crystals show Carlsbad twinning. We noted no primary plagioclase, although there is plagioclase in some of the lithic fragments, and plagioclase and biotite are in two hornblende dacite pumice clasts. Submicroscopic alkali feldspar may be present as a devitrification product. Again, we noted a few small opaque oxides, Fe-augite, and fayalite crystals in each sample, plus one or two grains of chevkinite and apatite in some samples. The Fe-augite to fayalite ratio is about 4:1. The relative abundances of phenocryst phases in units Qbt₁ and Qbt₂ at GC are similar to those documented in the broader Tshirege Member by Broxton et al. (1995), Stimac et al. (2002), and Goff et al. (2014, table 3, based on 221 thin sections).

X-ray Diffraction Analyses: Results of XRD analyses are listed in SD3. Within the GC area, we analyzed unaltered Qbt₂ from an outcrop above and away from GC proper and relatively unaltered Qbt₁ from an outcrop along FS10 (Fig. 3) between columns of highly altered Qbt₁ (numbers 1 and 5 in SD3). These relatively unaltered samples have roughly 11% to 14% quartz and 16% to 18% total alkali feldspar (sanidine plus albite). Significantly, they still contain 67% to 72% glass, very minor cristobalite and tridymite (≤0.3%), and essentially no zeolite alteration (0.5% mordenite). For comparison, two XRD analyses of Qbt₂ from a borehole and a measured section on the Pajarito Plateau in the Los Alamos area (numbers 2 and 3 in SD3) contain slightly more quartz, but more than 60% total alkali feldspar and absolutely no fresh glass. They also contain ≥20% cristobalite plus tridymite.

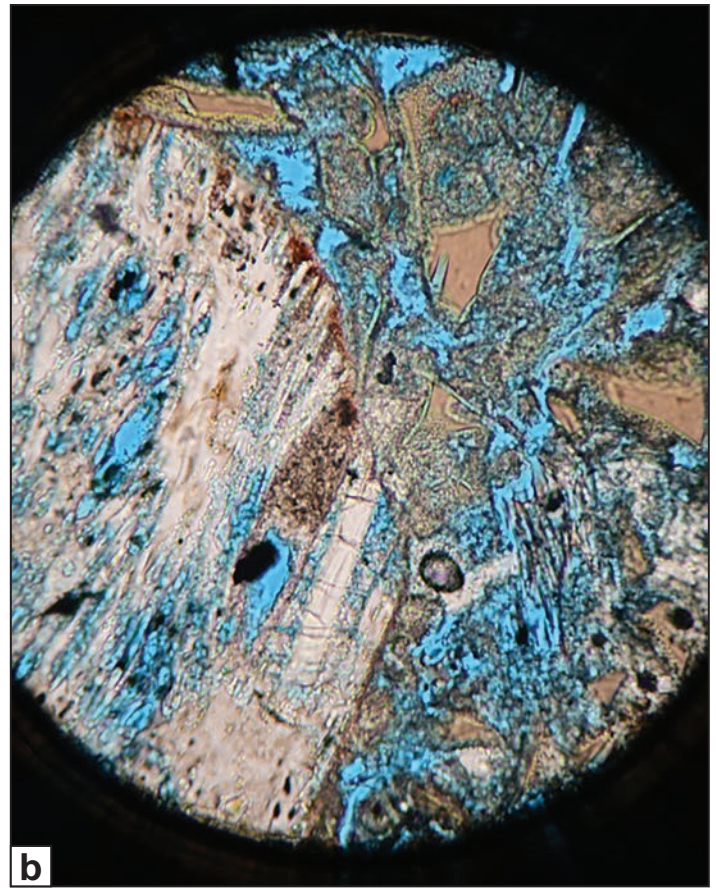
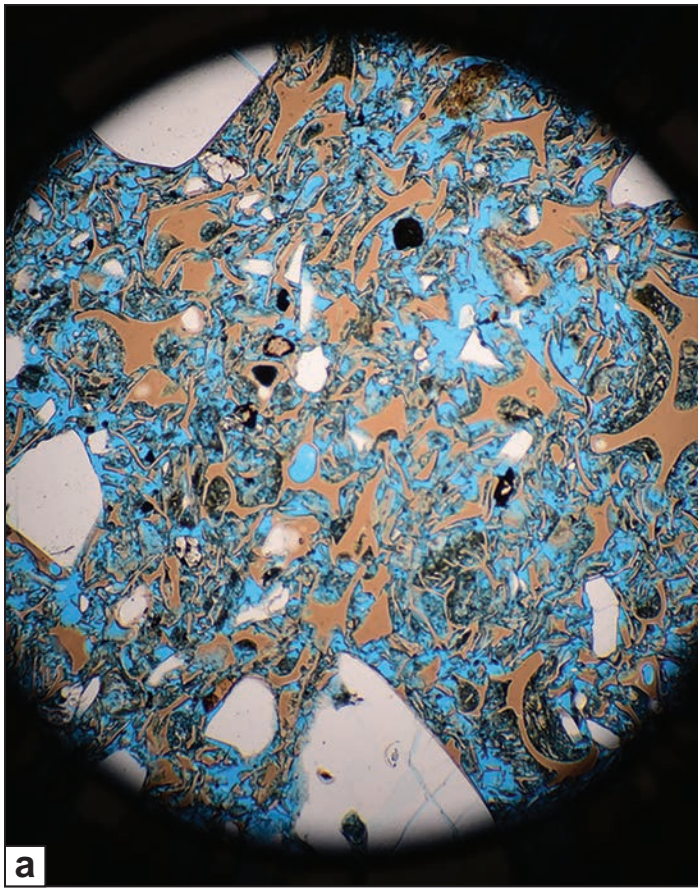


Figure 11. Photomicrographs in transmitted light from samples of glass-rich Tshirege ignimbrite. **a)** Sample F21-10 (Qbt_2) from the GC area at low power (field of view [FOV] about 5 mm). Glass shards are brown, voids and vesicles are blue epoxy, white crystals are quartz and alkali feldspar, black equant crystals are opaque oxides (ilmenite and titanomagnetite), and black dusty masses around brown glass shards are fine volcanic ash. Note that glass has sharp outlines because it is not altered. **b)** Sample F21-Gob1a (Qbt_1) from an altered column along FS10; FOV = 2 mm (medium power). Pumice patch on left is nearly replaced with white zeolite, and brown glass shards have fuzzy outlines due to zeolite replacement of glass and ash. Reddish-brown discoloration is secondary hematite.

According to Broxton et al. (1995) and Stimac et al. (2002), the exceptionally high total alkali feldspar, cristobalite, and tridymite are due to vapor-phase alteration of the tuff after emplacement at high temperatures, probably greater than 400°C (Smith and Brown, 1988). Apparently, unaltered tuff in the GC area cooled rapidly to temperatures below 400°C before most vapor-phase alteration could take place.

Near the base of Qbt_1 at GC, a few meters above the Tsankawi Pumice, a sample from the tabular ledges area (number 10 in SD3) contains similar amounts of quartz, total alkali feldspar, glass, cristobalite, and tridymite, as do the relatively unaltered Qbt_1 and Qbt_2 samples discussed above. For comparison, two XRD samples reported by Broxton et al. (1995) and Stimac et al. (2002) for Qbt_1 at the bottom of the Tshirege (numbers 11 and 12 in SD3) have on average similar quartz, total alkali feldspar, and high glass contents, and minimal if any cristobalite and tridymite. Apparently, basal Qbt_1 quenched so quickly on cold country rock that little if any vapor-phase alteration could occur, no matter the location.

The big differences between altered GC Tshirege (numbers 4, 6, 7, 8, 9, and 10 in SD3) and high-temperature devitrified Tshirege (numbers 2 and 3 in SD3) are the presence of zeolite

minerals, high glass contents, and low cristobalite and tridymite concentrations in the former, and the lack of zeolite minerals and glass, and much higher amounts of cristobalite and tridymite, in the latter. The mordenite and clinoptilolite formed mainly by reaction with glass, but the reactions have not gone to completion and significant glass remains. Zeolite formation does not substantially change the contents of primary (total) alkali feldspar. Interestingly, GC samples with the most zeolites (as much as 18%) seem to occur near the top of Qbt_1 or the edges of steam pipes in the middle of the unit (steam pipes are described in more detail below).

Mordenite can form at temperatures as high as 200°C in hydrothermal systems (Barger and Keith, 1995; Chipera and Apps, 2001; Chipera et al., 2008; Stimac et al., 2014, fig. 46.5). Mordenite and clinoptilolite are common constituents in low-temperature altered rocks in intracaldera lakes (Utada et al., 1999; Utada, 2001). In a previous study of low-temperature hydrothermal alteration within the Valles Caldera, Chipera et al. (2007, 2008) found both mordenite and clinoptilolite in intracaldera sediments and tuffs near the top and margins of the resurgent dome, indicating formation temperatures of $\leq 100^\circ\text{C}$. These zeolites were formed in the first intracaldera lake. Mordenite was generally most common in altered tuffs.

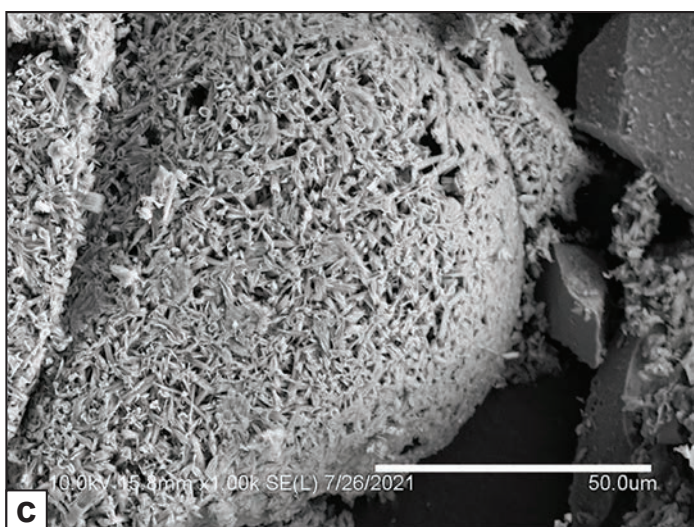
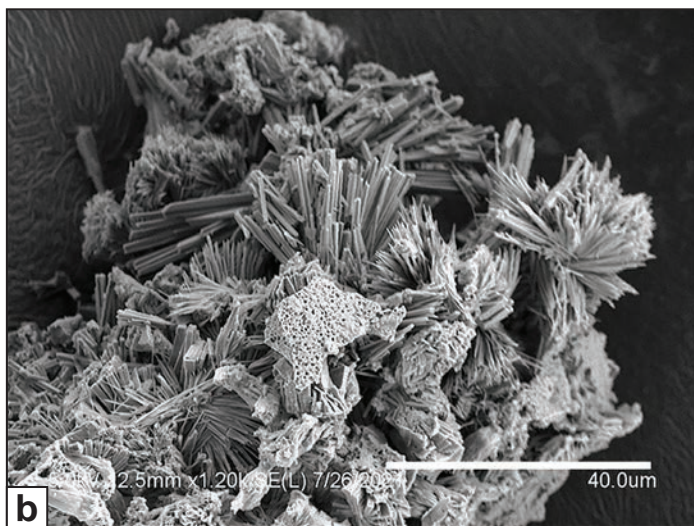
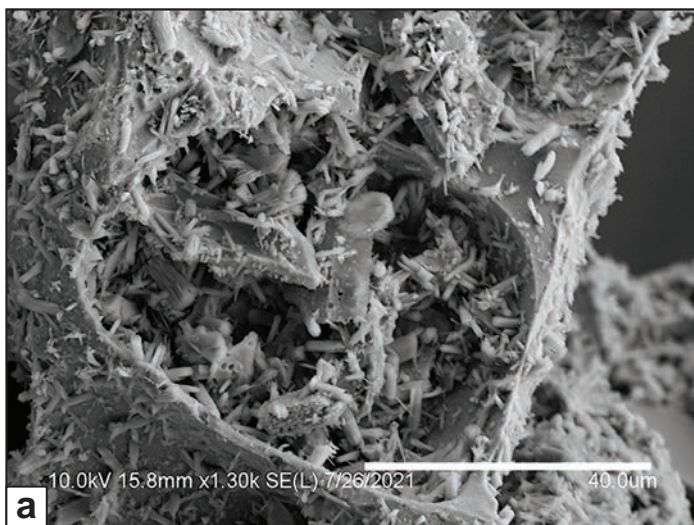


Figure 12. SEM images of altered Tshirege ignimbrite. Scale bars are 40 μm (12a and 12b) and 50 μm (12c). **a**) Broken, heart-shaped vesicle in a glass shard, sample F21-Gob1a. Tiny zeolite crystals line the walls of the vesicle. **b**) Pumiceous ash fragment surrounded by a multitude of zeolite sprays, mostly mordenite, sample F21-17. **c**) Vesicle lining from broken glass bubble showing ball-shaped development of tiny zeolite crystals, sample F21-Gob3.

Scanning Electron Microscope Images: We obtained SEM images from the glass and ash component of several samples analyzed by XRD and reported in SD3. Figure 12a shows a photo of a broken vesicle in a glass fragment from the top of Qbt_1 in the columns along FS10 (Fig. 3). Note the stubby prisms and whiskers of zeolite growing within and outside the vesicle. These crystals are mordenite; larger blocky crystals may be clinoptilolite. Scanning electron microscope energy dispersive spectroscopy analysis was performed on the two phases, but the results were inconclusive. Figure 12b shows abundant acicular crystals of mordenite around a fragment of pumiceous ash from a sample of Qbt_1 at the top of south wall (Fig. 8e). The tiny vesicles in the pumice are notable. Blockier crystals are probably clinoptilolite. Figure 12c shows a vesicle lining of fine mordenite and clinoptilolite within ash and pumice at the edge of a steam pipe midway in the Qbt_1 deposit, with notable ball-shaped form of the vesicle lining. Large crystals at the right in the photo are sanidine that have a few small zeolite crystals growing on their surfaces. Zeolite formation is particularly focused on the reactive volcanic glass and ash of Tshirege unit 1. Primary alkali feldspar and quartz appear to host very little zeolite formation.

Whole-Rock Chemistry: Seven major element analyses of Tshirege Member samples are listed in SD1. Five analyses are from the GC area and are compared with two analyses of fresh tuff from detailed borehole studies conducted previously on the Pajarito Plateau east of Los Alamos (Stimac et al., 2002). In general, the altered to unaltered GC Tshirege samples have similar chemistry to fresh samples. Most GC samples contain substantially more loss on ignition (LOI; in this case, primarily water) and slightly less SiO_2 and Na_2O , but slightly more Al_2O_3 and total iron as Fe_2O_3 than fresh Tshirege. Notably, GC Tshirege generally has slightly more CaO and noticeable additions of MgO and P_2O_5 . Fresh Tshirege has 0.00 weight percent (wt%) MgO and P_2O_5 . Both TiO_2 and MnO are roughly equivalent. Increases in total Fe_2O_3 , CaO, MgO, and P_2O_5 probably originate from alteration/deposition by postemplacement near-surface groundwater of some type. Decreases in SiO_2 and Na_2O could be due to postemplacement leaching and/or formation of zeolites.

To better compare results, we normalized the seven Tshirege analyses to 100% without LOI (SD2). The normalized analyses show more consistent chemical trends, although some trends are subtle. Goblin Colony samples generally show higher Al_2O_3 and total Fe_2O_3 , MgO, CaO, K_2O , and P_2O_5 concentrations (flagged in red in SD2) and, in contrast, are slightly lower in SiO_2 and Na_2O (flagged in blue in SD2). Again, TiO_2 and MnO are more or less unaffected. Excess total Fe_2O_3 , MgO, CaO, and P_2O_5 probably originates from hydrothermal fluid (hot water) rising from sediments and the intermediate-composition volcanic cobbles they contain, and from dacitic to basaltic rock below the tuff. Silica is easily leached by water flowing through glass-rich tuffs, but alumina is relatively immobile in water; thus, SiO_2 depletion results in apparent Al_2O_3 enrichment. The Al_2O_3 resides in residual feldspars and in postemplacement zeolites. Sodium is consistently depleted in the GC samples, although Na remains in primary feldspar and in newly formed zeolites.

Except for one sample (F21-Gob1a), K_2O is relatively enriched in GC samples compared with fresh Tshirege. Again, K_2O will remain in primary feldspar, but K_2O in glass will react with water to form zeolites.

Drone Survey

We conducted an aerial drone survey in GC to get a better understanding of structural trends and cluster patterns. For this task, we used DJI Mini 2 and EVO Autel 1 drones flown by a licensed operator (coauthor Gindreau). Drones lifted off and landed in clearings among the rock features, and stayed less than 130 m above land surface. To aid with location, we constructed four ground control points of removable colored cardboard that were located by portable GPS. The DJI Mini 2 was used to make vertical photos of the underlying terrain. The EVO Autel 1 was used to make movies by means of a panning camera to obtain gimbal views. Well over a hundred photos and several short videos were taken (<https://youtu.be/k1sz6k5MuSs>, <https://youtu.be/F9qSMGXfgp4>, <https://youtu.be/sl2jIYAzNLE>). Flying conditions were overcast and windless.

Several interesting observations can be made based on these images. First, a great many of the goblins in the main cluster and elsewhere are not simply round cylinders or spires; rather, many are broad fins, curving fins, and linear fins. The fins (Fig. 13a) occupy domains with preferred orientations transverse to the primary northeast trend of the main cluster. Some of the domains form a Y-shaped pattern pointing in a south to southeast direction. A second observation is that some of the features are concentrated into mazes with dark canyon-like interiors (Fig. 13b). In general, features within mazes show a preferred orientation, but not all features follow this pattern. A third observation is that the walls are not straight, they are segmented. The north wall curves and undulates and is cut by joints and open cracks that have preferred orientations, many to the northwest (Fig. 13c). The walls are about 15 to 25 m wide. The east end of the south wall has two prominent, northwest-trending en echelon fractures or faults (red lines, Fig. 13d). Clearly, all these features served as conduits for circulation of near-surface water (low-temperature hydrothermal fluids) that reacted with glass in the original tuff to form zeolites.

Significant Alteration and Erosion Features

Columns and Vertical and Subhorizontal Steam Pipes: The columns exposed along FS10 (Fig. 3) resemble leaning trees or logs to many first-time observers. The cores of the columns are softer than their rinds. Although we have looked at several scales, we could find no evidence of carbon residues or tree rings within the samples we collected. In the deep ravine between the north and south walls, the south face of the north wall displays a great number of log-like or tree stump protrusions that all tilt at high angles of roughly 60° to the north (Fig. 14a). Most of these columns have crude circular textures reminiscent of growth rings in cross sections of living trees (Figs. 14b and 14c). Diameters vary from 0.25 to 1.0 m. Although we looked for organic textures and carbon in thin sections of this material, we could not identify any organic fabrics or carbon residues.

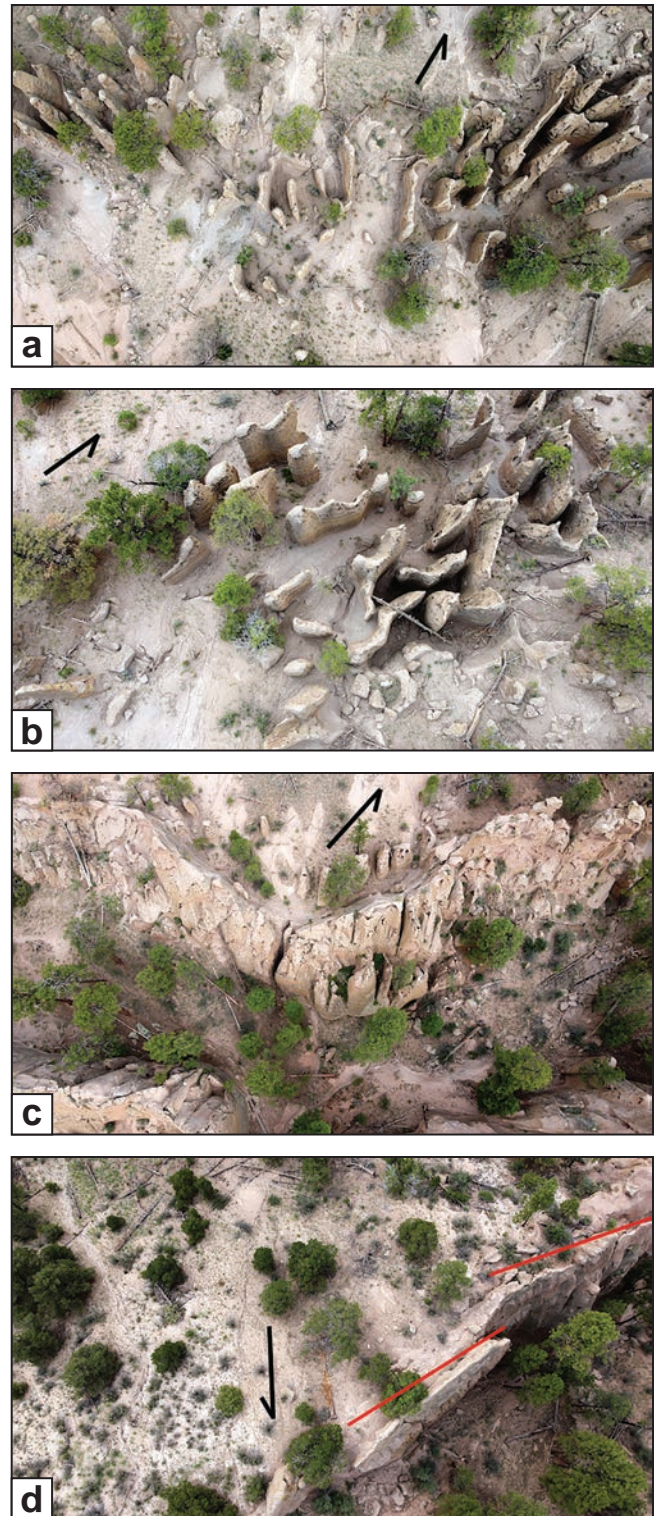


Figure 13. Drone images of GC. **a)** Goblins in the heart of the main cluster; arrow points north. Drone elevation above ground surface is roughly 30 m. Although there are isolated roundish spires, many of the goblin features are long, straight, and/or curving fins. **b)** A maze of curving fins and spires in the main cluster; arrow points north. Drone elevation about 30 m above surface. **c)** Southward undulation or bend in north wall; arrow points north (upslope; see Fig. 8a). The undulation is relatively symmetrical. Note the fractures and joints that crosscut the wall, and the deep ravine separating the north and south walls. **d)** Two subparallel en echelon fractures (or faults?) cutting the northeast end of the south wall (marked by red lines); arrow points north. Ravine between north and south walls is to the right. Note the blanket of white El Cajete pumice to the left side of the photo (see Fig. 8a).



Figure 14. Photos of steam pipes. **a)** Steam-pipe cluster that dips at an angle of about 60°, from the bottom south face of the north wall, located near the pipes shown in Figure 14b. Diameters of the pipes vary. The pipes are best exposed in the deep ravine between north and south walls. **b)** Steam pipe in the forested ravine of the south face of the north wall; hammer handle is 46 cm long. Samples F21-Gob2 and F21-Gob3 were collected from this pipe (SD3). Location of pipe is UTM NAD27 3954564N, 0353509E, elevation approximately 2,200 m. **c)** Cross section of steam pipe; sample F21-Gob5 is from the center (SD3).

XRD results of three samples (SD3) reveal that the rind of one steam pipe contains considerably more zeolitic alteration than the cores of two steam pipes, which contain only minor mordenite. This indicates that the cores of the steam pipes transported more water, probably as steam, than the rinds. Possibly, steam condensed into liquid water in the rinds, which is more reactive to host tuff. In any event, if these features are casts, which represent the charred and altered remains of trees, their presence has implications for the original pyroclastic flow velocity and other emplacement parameters (e.g., density) for the Tshirege Member ignimbrites at GC.

Ledges: The GC area with tabular ledges displays two shelves of more erosion-resistant tuff that dip gently to the southwest at about the same inclination as the Paliza Canyon tributary. These ledges are present in the lower part of Qbt_1 and can be traced into the lower elevations of the east cluster of features at GC (Figs. 8a and 15). The ledges are typically 7 to 15 cm thick. Sample F21-16 (SD3), from the upper ledge in the tabular ledges area, contains some hydrothermal mordenite and clinoptilolite but not as much as some other samples higher in the section. We do not know the precise origin of these ledges, but they are reminiscent of zeolitized paleowater tables described in the Tshirege Member on the Pajarito Plateau (Bailey and Smith, 1978; Goff et al., 1996, p. 71–73). In the latter paper, the primary zeolite is identified as clinoptilolite.

Erosion Cavities: The wall faces at GC display many subparallel lines of erosion cavities that appear to dip at about the same angle as the present ground surface (Fig. 8e). Similar cavities also occur in some of the spires and fins (Figs. 8b–d). We do not know the exact origin of these lines of cavities, but we postulate that they may be paleoground surfaces at which erosion stabilized for some period of time before subsequent erosion to a new level. The oldest lines of cavities are at the top. Another possibility is that the



Figure 15. Ledge near base of unit Qbt_1 (looking northwest), exposed in east cluster area (Fig. 8a) along the Paliza Canyon tributary. These ledges are moderately zeolitized and dip slightly to the southwest. Location is UTM NAD27 3954526N, 0353716E.

erosion lines mimic primary depositional boundaries in the tuff, but we do not observe any changes in bedding angle or thickness that parallel the lines. In any event, these cavities are erosional and postdate formation of the fumarolic features at GC.

Discussion

Geomorphic and Hydrologic Controls: Rocks at GC occupy a unique geomorphic and hydrologic setting. Apparently, a relatively small but deep, elongate canyon or basin with a southwest trend was eroded through the Otowi Member into older sedimentary and igneous rocks of the PCF. Southwest-northeast-trending dikes, plugs, and flows formed a buttress to erosion on the southeast margin of the canyon. The intrusive rocks at GC are dense, aphyric, and ≥ 30 m wide and formed a linear dike zone about 1.5 km long. We postulate that finer-grained sediments, possibly lacustrine or marsh deposits, occupied the bottom of the canyon along this dike zone when the Tshirege Member was erupted. It is also possible that cold springs issued into the canyon due to changing hydrology adjacent to the dike zone. About 100 m of Tshirege Member suddenly filled the GC basin at 1.23 Ma, disrupting the existing drainage system. Alteration of the tuff began immediately thereafter, and drainage out of GC was eventually recut toward the present position of the Paliza Canyon tributary.

High-Temperature Devitrification Versus Degasification:

Ash-flow tuff sheets (ignimbrites) such as the Bandelier Tuff are subject to several types of postemplacement gas release processes and alteration. The most widespread process is vapor-phase crystallization and devitrification (deuteric alteration) during cooling of the tuff sheet. Most researchers consider that volatile components dissolved in the original magma are the fundamental altering agent (e.g., Ross and Smith, 1960, p. 44; Cas and Wright, 1987, p. 258). In such cases, tridymite, cristobalite, and microcrystalline alkali feldspar form during cooling at the expense of primary glass at temperatures $\geq 400^\circ\text{C}$. This type of deuteric, vapor-phase alteration is pervasive in the central to upper zones of outflow sheets of Tshirege Member on the Pajarito Plateau (e.g., unit 2 in SD3, numbers 2 and 3; see also Broxton et al., 1995, fig. 5; Stimac et al., 2002, fig. 6). At GC, basal unit 2 of the Tshirege displays very little vapor-phase alteration (number 1 in SD3), $< 0.3\%$ each of cristobalite and tridymite, and no excess alkali feldspar. Significantly, basal unit 2 samples at GC and the Pajarito Plateau contain no zeolites.

Several other gas-release processes affect welded tuff sheets after emplacement, but they are generally smaller in scale and vertically oriented, crosscutting the depositional fabric of the tuff. These include fumarole mounds (Sheridan, 1970) and a variety of gas escape structures (gas-escape pipes, vapor-phase pipes, steam pipes, fumarolic pipes, and elutriation pipes; Fischer and Schmincke, 1984, p. 200). The former are as much as 60 m wide whereas the latter are generally a few meters to a few centimeters in diameter. Because of the diversity of these features, postulated mechanisms of growth, temperatures of formation, and sources of fluids vary considerably (Cas and Wright, 1987; Keating, 2005; Randolph-Flagg et al., 2017; Lipman, 2018; Pacheco-Hoyos et al., 2020). Fumarolic mounds have not been identified in the Bandelier Tuff,

but a variety of other gas-escape structures are known in both the Tshirege and the Otowi members (Crowe et al., 1978; Self et al., 1996; Caporuscio et al., 2012; F. Goff, unpublished locations).

Caporuscio et al. (2012) investigated a set of unique relict fumarole pipes in the Tshirege Member on the Pajarito Plateau near Los Alamos. The zone of pipe formation occurs within a few square kilometers, and pipes formed only within units Qbt₃ and Qbt₄ (see Goff et al., 2014, fig. 3 for Tshirege stratigraphy), well above the base of the ignimbrite. The pipes are less than a few meters wide, are fines-depleted, have distinctly flared tops, and create breccia zones within Qbt₄. The alteration mineral assemblage is deuteric in style, containing tridymite, cristobalite, secondary alkali feldspar, and marialite (a Na- and Cl-rich scapolite stable at higher temperatures). No zeolites were identified. Similar scapolite has been identified elsewhere in the Bandelier Tuff (Smith and Dickson, 1965). Because the pipes grew vertically within the upper part of the ignimbrite stack, it is logical to assume that the volatiles creating the pipes emanated solely from within the tuff. Caporuscio et al. (2012) argue that the causative fluids were high temperature and acidic, and provide strong comparisons of their pipes in the Tshirege to fumarole mounds developed within the Bishop Tuff and fumarole pipes formed in the ignimbrite sheets at Valley of Ten Thousand Smokes (VTTS), which were also high temperature and acidic (Sheridan, 1970; Griggs, 1922; Keith, 1991).

Within both Otowi and Tshirege members of the Bandelier Tuff, a gradation seems to exist between high-temperature fumarole pipes with distinctly flared tops and moderate fines-depletion, and elutriation pipes that are less flared and contain substantially more lithic fragments due to extreme fines-depletion caused by jetting steam. The first author has documented several locations of each type during many years of mapping and geochemical studies in the Jemez Mountains (e.g., Figs. 16a–16d). In each case, the pipes occur in restricted zones of < 200 m width within the ignimbrite sheets. At several locations the tuffs rest on gravels, suggesting that minor amounts of water in the underlying saturated gravels possibly contributed to magmatic water released from the tuffs to form the pipes. A spectacular example is found on the southeast margin of Oaks Mesa (16 km south southeast of Valles Caldera, Fig. 1) where the Tshirege Member overlies gravels filling a paleoravine that cut into the underlying Otowi Member. There, a swarm of > 100 vertical elutriation pipes as much as 50 m tall and ≤ 30 cm wide extends to the top of unit 1 (Fig. 16a). It is not clear if these pipes are restricted solely to unit 1 because unit 2 is eroded away. The pipes are enriched in lithic fragments (fines depleted) and pipe walls are quite distinct. The residual fine material within four samples of the pipes contains $\leq 6\%$ tridymite, $\leq 13\%$ cristobalite, and $\leq 58\%$ alkali feldspar, indicating that high-temperature (mostly magmatic?) fluid jetted vertically through the pipes. Quartz phenocrysts have been preferentially removed by jetting steam, and $\leq 4.6\%$ quartz remains. As much as 15% soft white opal-CT partially fills voids in the pipes. Glass contents are variable ($\leq 40\%$) depending on whether residual pumice and/or ash was entrained in the sample. In contrast, matrix tuff surrounding the pipes contains 0.6% tridymite, 0.0% cristobalite, 0.0% opal-CT, 9.9% quartz, 12.6% alkali feldspar, and 71.4% glass (F. Goff and S. Chipera, unpublished data, 2000).



Figure 16. Photographs of gas-escape pipes in Bandelier Tuff. **a)** Unit 1, Tshirege Member on the southwest edge of Oaks Mesa (OM in Fig. 1) showing a cluster of gas-escape pipes near the eroded top of the tuff. Location is UTM NAD27 3951662N, 0367602E at about 2,165 m elevation. **b)** Four pipes from the same general Oaks Mesa locality as Figure 16a. Two pipes are merging into one on the right side of the photo. The fine-grained material in these pipes contains significant tridymite, cristobalite, and secondary alkali feldspar (F. Goff and S. Chipera, unpublished data, 2000). **c)** Upward-flaring pipe (outlined by black dashed lines) in the top of the Otowi Member in lower cliff face west of upper Frijoles Canyon (FR in Fig. 1), about 3.2 km southeast of Valles Caldera rim. The top surface of the Otowi undulates due to erosion and is covered with surge deposits at the base of the younger Tshirege Member. Note the concentration of lithic fragments at the top of the pipe, which consist mostly of Paliza Canyon intermediate-composition rocks (Goff et al., 2011; Kelley et al., 2013b). This pipe is one of at least 30 at this location. The composition of the fine material has not been studied. Location is UTM NAD27 3966298N, 0372228E at an elevation of about 2,652 m. **d)** Several slender, lithic-rich gas-escape pipes in the middle of the Otowi Member, east side of Eagle Canyon (EA in Fig. 1; UTM NAD27 3951670N, 0375974E, about 1,845 m elevation). The pipes are approximately 30 m above the base of the tuff that rests on a well-exposed deposit of Neogene volcanoclastic gravel of the Cochiti Formation (Smith and Lavine, 1996). Note the concentration of lithic fragments, mostly Paliza Canyon andesite, caused by steam elutriation of fine particles (see Pacheco-Hoyos et al., 2020 for descriptions and photos of similar pipes). The composition of the fine material has not been studied, but some pipes are so indurated that they stand several centimeters above the surrounding tuff.

Low-Temperature Interactions of Ignimbrite with Surface

Water: Because Tshirege unit 1 ignimbrite (Qbt₁) at GC shows interaction with surface water, we present other examples of this phenomenon. A remarkable example of low-temperature interaction of rhyolitic ignimbrite with cold surface water is exposed along Lake Crowley in California in the 0.764 Ma Bishop Tuff (Randolph-Flagg et al., 2017, fig. 3). The authors postulate that ignimbrite ponded against the wall of the newly formed Long Valley Caldera and was overrun by a lake of cold water. Downward percolation of meteoric water eventually formed hundreds of evenly spaced columns tens of meters tall over an area of a few square kilometers. According to the authors, the only difference between altered tuff in columns and unaltered tuff surrounding columns is precipitation of secondary mordenite, which reacts primarily with glass. No other XRD data are presented. Hildreth and Fierstein (2017) and Lipman (2018) challenged this explanation, arguing that the water altering the tuff rose as steam from underlying water-saturated sediments in the valley where the ignimbrite was deposited.

Crowe et al. (1978, fig. 7) described columns of altered Otowi ignimbrite resembling those at GC in a small area of Pueblo Canyon southeast of Los Alamos. In this case, the Otowi overlies gravels of the Plio-Pleistocene Puye Formation. No XRD analyses were performed on the column material. Similar-looking columns are shown by Schmincke (2004, fig. 11.12) in an A.D. 965 trachyte ignimbrite exposed for several kilometers in a paleovalley of the Yalu River in North Korea. Again, no XRD data are presented describing the alteration, but the visual similarity to GC columns is striking.

Wright (1981) described eroded cylindrical steam pipes covering a small area in the rhyolitic Rio Caliente ignimbrite, La Primavera volcano, Mexico (Cas and Wright, 1987, fig. 8.46). In this occurrence, the features protrude near vertically ≤ 1.5 m above ground surface and look surprisingly similar to the steam pipes we have described at GC where the cores of the pipes are softer and more erodible than the rinds (Figs. 14b and 14c). The secondary cementing agents in the Rio Caliente pipes are predominately clinoptilolite and heulandite (another Ca-, K-, and Na-bearing low-temperature zeolite). Cas and Wright (1987, p. 259) state that this type of zeolite alteration would be “expected if the ignimbrite was locally deposited in a shallow lake or on marshy ground and vaporized groundwater was important.”

Stability of Hydrothermal Mordenite, Clinoptilolite, and Heulandite in Silicic Tuffs: Mordenite, clinoptilolite, and heulandite are common replacement minerals of silicic glass in water-saturated volcanic tuff at ambient to moderate-temperature hydrothermal conditions (Boles, 1977; Chipera and Apps, 2001; Chipera et al., 2007, 2008; Stimac et al., 2014, fig. 46.5). Stimac et al. (2014), drawing on extensive borehole data, show that mordenite is stable to 160°C, possibly as high as about 200°C. Barger and Keith (1995) found that mordenite was stable from 60° to 200°C in drill cores from rhyolite in Yellowstone National Park. Clinoptilolite is more stable at temperatures ≤ 100 °C, particularly at near surface pressures (Carey and Bish, 1996, fig. 9; Benning et al., 2000). Neutral to slightly alkaline

conditions (pH about 7 to 10) favor zeolite growth. The phase stability of mordenite and clinoptilolite in post-Valles Caldera tuffs and sediments has been discussed extensively by Chipera et al. (2007; 2008, fig. 9). These authors show that the association mordenite–clinoptilolite is highly favored in amorphous silica-saturated conditions at 25° to 99°C (i.e., in the presence of glass), and heulandite–clinoptilolite is favored in quartz-saturated fluid conditions at similar temperatures.

Mordenite is the only zeolite identified in pipes of altered Bishop Tuff (that formed during interaction of ignimbrite with cold water; Randolph-Flagg et al., 2017), whereas clinoptilolite–heulandite formed in the steam pipes of the Rio Caliente ignimbrite from vaporization of underlying near-surface water (Cas and Wright, 1987). Heulandite has not been identified in altered tuffs in either intracaldera Valles deposits or the altered tuffs at GC.

Within Valles Caldera, electron microprobe analyses of mordenite and clinoptilolite show that Ca²⁺, Na⁺, and K⁺ are the dominant cations, although clinoptilolite can contain some Mg²⁺ (Chipera et al., 2007; 2008, table 2). In mordenite, Na is greater than K, but in clinoptilolite K is greater than Na. In a setting such as this, where intracaldera lake water has interacted with tuffs and sediments, mordenite is more common in the tuffs (Na- and K-rich) and clinoptilolite is more common in the sediments that include relatively Ca-rich precaldera volcanic detritus. In the Na- and K-rich tuffs at GC, mordenite is the dominant zeolite (SD3). Ratios of mordenite to clinoptilolite generally range from 5:1 to 2:1; clinoptilolite is absent in two samples from steam-pipe cores (temperature ≤ 200 °C). Calcium oxide in fresh Bandelier Tuff is usually ≤ 0.3 wt% of bulk tuff (SD1 and SD2). Thus, the presence of excess calcium in altered GC ignimbrites (as much as 0.97 wt% CaO) is compelling evidence that water—either as liquid or flashed into steam—has contributed to the formation of zeolites.

Temperature and Timing of Fluid Transport in Goblin

Colony Features: It is evident from our examination of altered Tshirege ignimbrite at GC that moderate-temperature fluids (temperature ≤ 200 °C) circulated in a variety of structures. These structures are rootless; they do not extend into the rocks beneath the ignimbrite. But which structures propagated first? Initial interaction of ignimbrite with water-saturated ground created boiling to near-boiling conditions that are well preserved in the central to upper portions of GC. It is our opinion that the steam pipes, especially pipe rinds, and columns formed first because they contain the most zeolites (SD3). With time, cooling and compaction, combined with later fracturing and localized faulting, created open cracks and broad walls that continued to precipitate zeolites, but in lesser quantities. Most of the zeolite-cemented features that form fins, mazes, spires, and walls formed while the deposit cooled and compacted. The altered shelves in the tabular ledges area seen near the bottom of GC exposures (Fig. 8e) were formed last when the deposit had lost most excess heat and cold meteoric water from rain and snow saturated the deposit. The altered tuff in postemplacement groundwater horizons should not be confused with vertical to subvertical columns and steam pipes of zeolite-altered tuff caused by instantaneous emplacement of hot tuff over surface water.

Comparisons with Valley of Ten Thousand Smokes: The eruption of Novarupta volcano, near Katmai, Alaska, in 1912 and subsequent creation of the VTTS (Griggs, 1922) provides some insights on events that occurred at GC at 1.23 Ma. Instantaneous emplacement of 11 to 13 km³ of silicic ignimbrite from Novarupta covered a broad, glacially carved valley with a 120-km² sheet that was roughly 15 km long. The average thickness of tuff was about 100 m. A 1916 expedition to the remote area led by Griggs eventually saw the “most amazing vision ever beheld by mortal eye,” an entire valley filled “with tens of thousands of smokes, curling up from its fissured floor” (Griggs, 1922, p. 191). Since then, numerous studies have been conducted at VTTS (e.g., Hildreth, 1983; Kodosky and Keith, 1995; Hogeweg et al., 2005; Hildreth and Fierstein, 2012). Although small by Valles Caldera standards, the Novarupta eruption was the largest of the twentieth century and the largest silicic eruption of the last millennium.

The VTTS ignimbrite covered streams, snow, and marshes, forming low- and high-temperature fumaroles and small phreatic explosion craters (Hogeweg et al., 2005). Many steam plumes rose to heights ≤600 m. In 1917, fumarole temperatures were ≤645°C (Allen and Zies, 1923). According to these authors, most of the gas was steam, 98.4% to 99.99% by volume, but residual components were HCl, CO₂, H₂S, CH₄, HF, CO, NH₄, and recycled air. Those who worked in the valley at that time remarked on the horrid odors released by the fumaroles. Most observers considered that the fluid was a mixture of water degassing from within the ignimbrite, water derived from underlying sediments, and meteoric water. Griggs (1922) noted that the tuff had rapidly compacted and that many fumaroles discharged from lines of cracks with many orientations within the ignimbrite. Although various fumarole incrustations were described, the mineral assemblage was consistent with high-temperature, acidic conditions (Kodosky and Keith, 1995). No zeolite minerals have ever been recognized. Fumarolic activity was essentially absent by the 1930s, although tepid hot spring activity persisted near the base of the ignimbrite until at least 2001 (Hogeweg et al., 2005).

The volume of VTTS ignimbrite is roughly 3% of the volume of the Tshirege Member (approximately 400 km³; Goff, 2009), yet the former filled an open valley at the base of the source vent. VTTS ignimbrite was emplaced rapidly, forming a welded tuff sheet that retained heat as hot as 645°C several years after eruption. In contrast, the Tshirege ignimbrite at GC traveled 11 km from the southern Valles Caldera rim over complex terrain and was emplaced at much lower temperatures. Most of the volatile components were probably lost and much air was probably entrained before emplacement of the tuff. Even though the GC deposit is roughly 100 m thick, there is no significant welding and virtually no vapor-phase alteration; thus, the initial emplacement temperature was probably no more than 400°C and probably much less. Instead of acidic or high-temperature deuteric alteration, mineral composition in the core of GC steam pipes, intuitively the hottest zones of degassing, consists of 64% to 66% glass and only 1.4% mordenite (SD3), whereas the rinds of the pipes contain 17% total zeolites, probably formed from reaction of condensed steam with the glass. Clearly, temperatures of GC fumaroles were much lower than those at VTTS. Whether hot

springs or warm springs evolved at the margins of the ignimbrite at GC is not known, but no hot spring deposits have been found. Based on observations at VTTS, GC fumaroles probably existed for fewer than 100 years, but hydrothermal circulation and zeolitic alteration persisted longer. The ledges at the bottom of GC exposures indicate that cold meteoric water reacted with tuff to produce zeolites many years after emplacement.

Conclusions

Fumarole monoliths, walls, and other formations at GC are different and more rare than typical gas-escape and/or elutriation pipes commonly seen in ignimbrite sheets (e.g., Pacheco-Hoyos et al., 2020). The latter are observed as swarms of pipes or upward-flaring pipes in localized areas and grow primarily in the tops of ignimbrites (or flow units). They are believed to form during outgassing of mostly magmatic water, but in some cases meteoric water may contribute to their formation. In both Otowi and Tshirege members of the Bandelier Tuff, high-temperature gas-escape/elutriation pipes are widely distributed (i.e., Figs. 16a–d; Caporuscio et al., 2012).

Our concept of geologic evolution and formation of the unusual altered rocks in the GC area is presented in Figure 17. Goblin Colony consists of a zone (0.15 km² or 37 acres) of zeolite-altered rhyolite ignimbrite (unit 1, Tshirege Member). A complex volcanic terrain of preexisting canyons, valleys, and ridges had developed in the region before eruption of the tuff. A small canyon with a southwest-flowing stream was carved into Miocene (10 to 7 Ma) volcanic rocks, and the canyon bottom probably included a pond or marsh and possibly cold springs. An impressive 1.5-km-long dike zone of mostly dacite (9 to 7 Ma) bounded the southeastern margin of the small canyon, creating an impermeable barrier to southwest-flowing drainage. When the Tshirege Member erupted from Valles Caldera (1.23 Ma), the pyroclastic cloud flowed 11 km over this complex terrain and filled the small canyon with about 100 m of tuff. Because the tuff is nonwelded to poorly welded and displays no high-temperature vapor-phase alteration, it was emplaced at temperatures well below 400°C. Interaction of hot tuff with cold surface water in the canyon created plumes of rising steam and hot water that formed temporary fumaroles that are expressed as pipes and columns. Interaction of hydrothermal fluids with tuff produced mordenite and clinoptilolite at the expense of rhyolitic glass. These two zeolites are stable at temperatures ≤200°C in mildly alkaline hydrothermal conditions (Barger and Keith, 1995; Chipera and Apps, 2001; Chipera et al., 2007, 2008; Stimac et al., 2014). As fumarolic activity waned, compaction, fracturing, and faulting of the tuff provided additional conduits for hydrothermal circulation, forming spires, fins, mazes, and walls of zeolite-laden tuff. Although all these features collectively form a broad northeast-southwest-trending structural zone, individual spires, fins, and mazes are randomly oriented. Fumaroles lasted no more than 50 years, but low-temperature hydrothermal activity may have persisted for another 100 years or more. Eventually, cold meteoric water saturated the bottom of the tuff sequence at GC, forming indurated tuff layers containing secondary zeolites at the top of the water table. Because zeolite-altered tuff is more resistant to weathering and erosion than nonwelded tuff, a new drainage

was established (the Paliza Canyon tributary) that exposed the 100-m-high section of altered tuff at GC and cut a notch through the dacite dike zone.

Our results and interpretations indicate that broad areas of zeolite-rich fumarole pipes and related features form when low-temperature ignimbrite deposits (temperature ≤ 400 °C) interact with external surface water and saturated substrates. A distal, gas-depleted environment characterized the ignimbrite at GC. Additional meteoric water infiltrated the tuff from above.

Conditions of formation were mildly alkaline and alteration temperatures were mostly ≤ 200 °C. If the ignimbrite is emplaced at high temperature on a preexisting wet substrate (as in the VTTS case), high-temperature fumaroles develop when the fluids are mixtures of meteoric water and small amounts of magmatic volatiles degassing from tuff. Resulting fluids are acidic, and coexisting mineral assemblages and deposits reflect high-temperature conditions. In either case, durations of fumarole outgassing and hydrothermal circulation are short, probably 100 to 200 years at most.

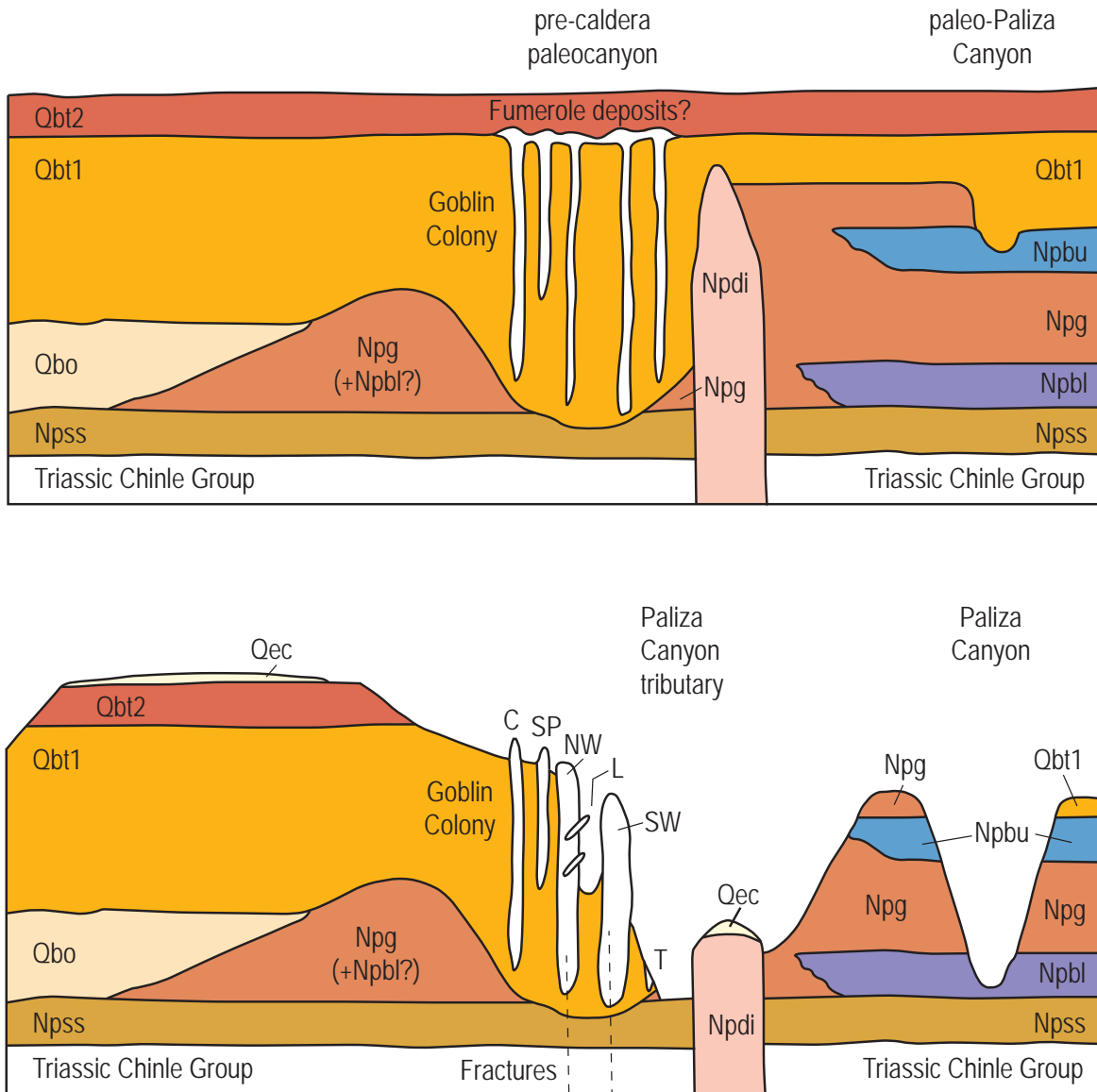


Figure 17. Diagrammatic illustrations showing the geologic and hydrothermal evolution of GC. Colors and names of geologic units are the same as Fig. 2 except for fumarolic structures that are depicted in white. Triassic Chinle Group is shown at bottom of section because it is exposed beneath unit Npg west of our map area (see Kempter et al., 2007). Vertical exaggeration is $>4:1$. The profile is generally oriented northwest to southeast across the Paliza Canyon tributary in Figure 2. **Top)** Time = 1.23 Ma. Voluminous ignimbrite of Tshirege Member covered an eroded and probably faulted landscape developed in the southern Jemez Mountains volcanic field. Emplacement temperature of Qbt₁ (unit 1) in this area is probably around 200°C. Unit 1 fills a previously developed paleocanyon that contained a pond, marsh, and possibly cold springs. Hot ignimbrite vaporized the surface water that rose to form discrete steam pipes and columns. Heated water and steam reacted with glass in the tuff to form mordenite, clinoptilolite, and low-temperature Fe-oxides. Possibly, fumarole deposits formed above the pipes and columns (i.e., Griggs, 1922; Caporuscio et al., 2012), but if so, the deposits were later eroded away. **Bottom)** Time = present day. Fractures developed early in the hydrothermal evolution of GC formed two walls of zeolite-altered tuff that enveloped previously formed pipes and columns (e.g., the tilted steam pipes in the north wall). The fractures shown may actually be small faults that disrupted and rotated initially formed steam pipes (e.g., Fig. 14a), as depicted here by the tilted steam pipes (L) in the north wall. Fractures and/or faults also formed en echelon offsets in south wall (e.g., Fig. 13d). Erosion cut a new drainage (Paliza Canyon tributary) that exposed the altered rocks that make up GC. Labels: C = column, SP = spire, T = tabular ledges, NW = north wall, SW = south wall, and L = deep ravine between the two walls, exposing rotated steam pipes submerged in north wall.

Acknowledgments

C.J. Goff thanks Anne Gartner (USGS, retired) for providing her personal copy of the 1922 monumental work on VTTS by Griggs. Gerardo Aguirre-Dias (UNAM, Queretaro, Mexico) graciously provided us with a paper on elutriation pipes in the Huichapan Ignimbrite. We also thank Steve Self, Jim Stimac, Robert Andres, and Greg Valentine for excursions in and around the Bandelier Tuff from 1982 to the present looking at ignimbrite and a variety of gas-escape pipes and related features. Warner Petrographic LLC, Lindon, Utah, prepared our thin sections. XRD analyses were obtained from the labs of Chesapeake Energy, Oklahoma City, Oklahoma. SEM photos and analyses were provided by the New Mexico Bureau of Geology and Mineral Resources (NMBGMR), Socorro, New Mexico. Whole-rock chemical analyses were purchased from ALS Global, Reno, Nevada. Bendt Dahl of Los Alamos, New Mexico, helped with the drone survey. Figures 2 and 17 were drafted by Shari Kelley and Phil Miller (NMBGMR). Field and analytical expenses were partially subsidized by the William H. Riley Fund (donated by D. Schiferl), the Ace Johnson Research Fund (donated by L. Waters), and personal investments of F. and C.J. Goff. We thank the Pajarito Environmental Education Center, Los Alamos, New Mexico, for their support. Reviews by Larry Crumpler (New Mexico Museum of Natural History and Science) and Shari Kelley (NMBGMR) greatly improved our draft manuscript. Bruce Allen (NMBGMR) handled the editorial requirements of review and publication.

Some of the data collected in this study are presented in Supplementary Data tables, which are available as separate, downloadable files at <https://geoinfo.nmt.edu/repository/index.cfm?rid=20230001>

References

- Allen, E.T., and Zies, E.G., 1923, A chemical study of the fumaroles of the Katmai region: National Geographic Society Contributions Technical Paper, Katmai Series, v. 2, p. 75–155.
- ALS Global, 2021, Schedule of services and fees: ALS Geochemistry, Reno, NV, 52 p.
- Bailey, R.A., and Smith, R.L., 1978, Volcanic geology of the Jemez Mountains, New Mexico: New Mexico Bureau of Mines and Mineral Resources Circular 165, p. 184–196. <https://doi.org/10.56577/FFC-12.139>
- Bailey, R.A., Smith, R.L., and Ross, C.S., 1969, Stratigraphic nomenclature of volcanic rocks in the Jemez Mountains, New Mexico: U.S. Geological Survey Bulletin 1274-P, 19 p. <https://doi.org/10.3133/b1274P>
- Barger, K.E., and Keith, T.E.C., 1995, Calcium zeolites in rhyolitic drill cores from Yellowstone National Park, Wyoming, *in* Ming, D.W., and Mumpton, F.A., eds., *Natural Zeolites '93—Occurrence, Properties, Use*: Brockport, NY, International Committee on Natural Zeolites, p. 69–86.
- Benning, L.G., Wilkin, R.T., and Barnes, H.L., 2000, Solubility and stability of zeolites in aqueous solution—II. Calcic clinoptilolite and mordenite: *American Mineralogist*, v. 85, p. 435–508. <https://doi.org/10.2138/am-2000-0411>
- Boles, J.R., 1977, Zeolites in low-grade metamorphic grades, *in* Mumpton, F.A., ed., *Mineralogy and Geology of Natural Zeolites*: Mineralogical Society of America Short Course Notes, v. 4, p. 103–135. <https://doi.org/10.1515/9781501508585-010>
- Boro, J.R., Wolff, J.A., and Neill, O.K., 2020, Anatomy of a recharge magma—Hornblende dacite pumice from the rhyolitic Tshirege Member of the Bandelier Tuff, Valles Caldera, New Mexico, USA: *Contributions to Mineralogy and Petrology*, v. 175. <https://doi.org/10.1007/s00410-020-01725-w>
- Broxton, D.E., and Reneau, S.L., 1995, Stratigraphic nomenclature of the Bandelier Tuff for the Environmental Restoration Project at Los Alamos National Laboratory, Los Alamos, New Mexico: Los Alamos National Laboratory Report LA-13010-MS, 21 p. <https://permalink.lanl.gov/object/tr?what=info:lanl-repo/lareport/LA-13010-MS>
- Broxton, D.E., Heiken, G.H., Chipera, S.J., and Byers, F.M., Jr., 1995, Stratigraphy, petrography, and mineralogy of Bandelier Tuff and Cerro Toledo deposits, *in* Broxton, D.E., and Eller, P.G., eds., *Earth Science Investigations for Environmental Restoration—Los Alamos National Laboratory Technical Area 21: Los Alamos National Laboratory Report LA-12934-MS*, p. 33–64. <https://permalink.lanl.gov/object/tr?what=info:lanl-repo/lareport/LA-12934-MS>
- Caporuscio, F.A., Gardner, J.N., Schultz-Fellenz, E.S., and Kelley, R.E., 2012, Fumarolic pipes in the Tshirege Member of the Bandelier Tuff on the Pajarito Plateau, Jemez Mountains, New Mexico: *Bulletin of Volcanology*, v. 74, 17 p. <https://doi.org/10.1007/s00445-012-0582-4>
- Carey, J.W., and Bish, D.L., 1996, Equilibrium in the clinoptilolite-H₂O system: *American Mineralogist*, v. 81, p. 952–962. <https://doi.org/10.2138/am-1996-7-817>
- Cas, R.A.F., and Wright, J.V., 1987, *Volcanic Successions, Modern and Ancient*: London, Unwin Hyman, 528 p. <https://doi.org/10.1007/978-94-009-3167-1>
- Chipera, S.J., and Apps, J.A., 2001, Geochemical stability of natural zeolites, *in* Bish, D., and Ming, D., eds., *Natural zeolites—Occurrence, properties, applications*: Mineralogical Society of America Reviews in Mineralogy, v. 45, p. 117–161. <https://doi.org/10.2138/rmg.2001.45.3>

- Chipera, S.J., and Bish, D.L., 2002, FULLPAT: A full-pattern quantitative analysis program for X-ray powder diffraction using measured and calculated patterns: *Journal of Applied Crystallography*, v. 35, p. 744–749. <https://doi.org/10.1107/S0021889802017405>
- Chipera, S.J., and Bish, D.L., 2013, Fitting full X-Ray diffraction patterns for quantitative analysis—A method for readily quantifying crystalline and disordered phases: *Advances in Materials Physics and Chemistry*, v. 3, p. 47–53. <http://doi.org/10.4236/ampc.2013.31A007>
- Chipera, S.J., Goff, F., Goff, C.J., and Fittipaldo, M., 2007, Zeolitization of intracaldera sediments and rhyolitic rocks in the Valles caldera, New Mexico: *New Mexico Geological Society Guidebook 58*, p. 373–381.
- Chipera, S.J., Goff, F., Goff, C.J., and Fittipaldo, M., 2008, Zeolitization of intracaldera sediments and rhyolitic rocks in the 1.25 Ma lake of Valles caldera, New Mexico, USA: *Journal of Volcanology and Geothermal Research*, v. 178, p. 317–330. <https://doi.org/10.1016/j.jvolgeores.2008.06.032>
- Crowe, B.M., Linn, G.W., Heiken, G., and Bevier, M.L., 1978, Stratigraphy of the Bandelier Tuff in the Pajarito Plateau: *Los Alamos Scientific Laboratory Report LA-7225-MS*, 56 p. <https://doi.org/10.2172/6870764>
- Deer, W.A., Howie, R.A., and Zussman, J., 1992, *An Introduction to the Rock Forming Minerals*, 2nd edition: Essex, Longman Scientific & Technical, 696 p. <https://doi.org/10.1180/DHZ>
- Fischer, R.V., and Schmincke, H.-U., 1984, *Pyroclastic Rocks*: Berlin, Springer-Verlag, 472 p. <https://doi.org/10.1007/978-3-642-74864-6>
- Gardner, J.N., 1985, Tectonic and petrologic evolution of the Keres Group: Implications for the development of the Jemez Volcanic Field, New Mexico [Ph.D. dissertation]: Davis, University of California, 293 p.
- Gardner, J.N., Goff, F., Garcia, S., and Hagan, R.C., 1986, Stratigraphic relations and lithologic variations in the Jemez volcanic field, New Mexico: *Journal of Geophysical Research*, v. 91, p. 1763–1778. <https://doi.org/10.1029/JB091iB02p01763>
- Gardner, J.N., Goff, F., Kelley, S.A., and Jacobs, E., 2010, Rhyolites and associated deposits of the Valles-Toledo caldera complex: *New Mexico Geology*, v. 32, p. 3–18. https://geoinfo.nmt.edu/publications/periodicals/nmg/32/n1/nmg_v32_n1_p3.pdf
- Goff, F., 1996, Vesicle cylinders in vapor-differentiated basalt flows: *Journal of Volcanology and Geothermal Research*, v. 71, p. 167–185. [https://doi.org/10.1016/0377-0273\(95\)00073-9](https://doi.org/10.1016/0377-0273(95)00073-9)
- Goff, F., 2009, *Valles Caldera—A Geologic History*: Albuquerque, University of New Mexico Press, 114 p.
- Goff, F., 2010, The Valles caldera—New Mexico’s supervolcano: *Earth Matters*, v. 10, no. 1, p. 1–4. https://geoinfo.nmt.edu/publications/periodicals/earthmatters/10/n1/em_v10_n1.pdf
- Goff, F., et al., 1996, Third-day road log, from Los Alamos through the southeastern Jemez Mountains to Cochiti Pueblo and the Rio Grande: *New Mexico Geological Society Guidebook 47*, p. 59–91. <https://doi.org/10.56577/FFC-47.59>
- Goff, F., Gardner, J.N., Reneau, S.L., and Goff, C.J., 2006, Geologic map of the Redondo Peak quadrangle, Sandoval County, New Mexico: *New Mexico Bureau of Geology and Mineral Resources Open-File Geologic Map OF-GM111*, scale 1:24,000. <https://geoinfo.nmt.edu/publications/maps/geologic/ofgm/details.cfm?volume=111>
- Goff, F., Gardner, J.N., Reneau, S.L., Kelley, S.A., Kempton, K.A., and Lawrence, J.R., 2011, Geologic map of the Valles caldera, Jemez Mountains, New Mexico: *New Mexico Bureau of Geology and Mineral Resources Geologic Map 79*, scale 1:50,000. <https://geoinfo.nmt.edu/publications/maps/geologic/gm/79/>
- Goff, F., Warren R.G., Goff, C.J., and Dunbar, N., 2014, Eruption of reverse-zoned upper Tshirege Member, Bandelier Tuff from centralized vents within Valles caldera, New Mexico: *Journal of Volcanology and Geothermal Research*, v. 276, p. 82–104. <https://doi.org/10.1016/j.jvolgeores.2014.02.018>
- Griggs, R.F., 1922, *The Valley of Ten Thousand Smokes*: Washington D.C., National Geographic Society, 340 p.
- Hildreth, W., 1983, The compositionally zoned eruption of 1912 in the Valley of Ten Thousand Smokes, Katmai National Park, Alaska: *Journal of Volcanology and Geothermal Research*, v. 18, p. 1–56. [https://doi.org/10.1016/0377-0273\(83\)90003-3](https://doi.org/10.1016/0377-0273(83)90003-3)
- Hildreth, W., and Fierstein, J., 2012, The Novarupta-Katmai eruption of 1912—Largest eruption of the twentieth century, centennial perspectives: *U.S. Geological Survey Professional Paper 1791*, 259 p. <https://pubs.usgs.gov/pp/1791/>
- Hildreth, W., and Fierstein, J., 2017, Geologic field-trip guide to Long Valley Caldera, California: *U.S. Geological Survey Scientific Investigations Report 2017-5022-L*, 119 p. <https://doi.org/10.3133/sir20175022L>
- Hogeweg, N., Keith, T.E.C., Colvard, E.M., and Ingebritsen, S.E., 2005, Ongoing hydrothermal heat loss from the 1912 ash-flow sheet, Valley of Ten Thousand Smokes, Alaska: *Journal of Volcanology and Geothermal Research*, v. 143, p. 279–291. <https://doi.org/10.1016/j.jvolgeores.2004.12.003>
- Holsapple, K., 2019, Prime Passages, Goblin Colony hike: <https://primepassages.com/goblin-colony-hike> (accessed April, 2023).
- Holsapple, K., 2021, Goblin Colony hike: <https://www.hikingproject.com/trail/7100245/goblin-colony-hike> (accessed April, 2023).
- Izett, G.A., and Obradovich, J.D., 1994, ⁴⁰Ar/³⁹Ar age constraints for the Jaramillo Normal Subchron and the Matuyama-Brunhes geomagnetic boundary: *Journal of Geophysical Research*, v. 99, p. 2925–2934. <https://doi.org/10.1029/93JB03085>
- Keating, G.N., 2005, The role of water in cooling ignimbrites: *Journal of Volcanology and Geothermal Research*, v. 142, p. 145–171. <https://doi.org/10.1016/j.jvolgeores.2004.10.019>
- Keefer, K.D., and Brown, G.E., 1978, Crystal structures and compositions of sanidine and high albite in cryptoperthitic intergrowth: *American Mineralogist*, v. 63, p. 1264–1273.

- Keith, T.E.C., 1991, Fossil and active fumaroles in the 1912 eruption deposits, Valley of Ten Thousand Smokes, Alaska: *Journal of Volcanology and Geothermal Research*, v. 45, p. 227–245. [https://doi.org/10.1016/0377-0273\(91\)90061-4](https://doi.org/10.1016/0377-0273(91)90061-4)
- Kelley, S., Goff, F., Gautier, R., and Rogers, M.A., 2007, Day 3 supplemental road log: New Mexico Geological Society Guidebook 58, p. 117–129. <https://doi.org/10.56577/FFC-58.117>
- Kelley, S.A., Kempter, K.A., McIntosh, W. C., Maldonado, F., Smith, G.A., Connell, S.D., Koning, D.J., and Whiteits, J., 2013a, Syndepositional deformation and provenance of Oligocene to Lower Miocene sedimentary rocks along the western margin of the Rio Grande rift, Jemez Mountains, New Mexico, *in* Hudson, M.R., and Grauch, V.J.S., eds., *New Perspectives on Rio Grande Rift Basins—From Tectonics to Groundwater: Geological Society of America Special Paper 494*, p. 101–124. [https://doi.org/10.1130/2013.2494\(05\)](https://doi.org/10.1130/2013.2494(05))
- Kelley, S.A., McIntosh, W.C., Goff, F., Kempter, K.A., Wolff, J.A., Esser, R., Braschayko, S., Love, D., and Gardner, J.N., 2013b, Spatial and temporal trends in pre-caldera Jemez Mountains volcanic and fault activity: *Geosphere*, v. 9, p. 614–646. <https://doi.org/10.1130/GES00897.1>
- Kempter, K.A., Osburn, G.R., Kelley, S.A., Rampey, M., Ferguson, C., and Gardner, J., 2007, Geologic map of the Bear Springs Peak 7.5-minute quadrangle, Sandoval County, New Mexico: New Mexico Bureau of Geology and Mineral Resources Open-File Geologic Map OF-GM74, scale 1:24,000. <https://geoinfo.nmt.edu/publications/maps/geologic/ofgm/details.cfml?volume=74>
- Kodosky, L.G., and Keith, T.E.C., 1995, Further insights into the geochemical evolution of fumarolic alteration, Valley of Ten Thousand Smokes, Alaska: *Journal of Volcanology and Geothermal Research*, v. 65, p. 181–190. [https://doi.org/10.1016/0377-0273\(94\)00117-Y](https://doi.org/10.1016/0377-0273(94)00117-Y)
- Lipman, P.W., 2018, When ignimbrite meets water—Megascale gas-escape structures formed during welding: *Geology*, v. 47, p. 63–66. <https://doi.org/10.1130/G45772.1>
- Nasholds, M.W.M., and Zimmerer, M.J., 2022, High-precision $^{40}\text{Ar}/^{39}\text{Ar}$ geochronology and volumetric investigation of volcanism and resurgence following eruption of the Tshirege Member, Bandelier Tuff, at the Valles caldera: *Journal of Volcanology and Geothermal Research*, v. 431, 107624. <https://doi.org/10.1016/j.jvolgeores.2022.107624>
- Osburn, G.R., Kelley, S.A., Rampey, M., Ferguson, C.A., Frankel, K., and Pazzaglia, F., 2002, Geologic map of the Ponderosa quadrangle, Sandoval County, New Mexico: New Mexico Bureau of Geology and Mineral Resources Open-File Geologic Map OF-GM57, scale 1:24,000. <https://geoinfo.nmt.edu/publications/maps/geologic/ofgm/details.cfml?volume=57>
- Pacheco-Hoyos, J.G., Aguirre-Diaz, G.J., and Davila-Harris, P., 2020, Elutriation pipes in ignimbrites—An analysis of concepts based on the Huichapan Ignimbrite, Mexico: *Journal of Volcanology and Geothermal Research*, v. 403, 13 p. <https://doi.org/10.1016/j.jvolgeores.2020.107026>
- Phillips, E.H., Goff, F., Kyle, P.R., McIntosh, W.C., Dunbar, N.W., and Gardner, J.N., 2007, The $^{40}\text{Ar}/^{39}\text{Ar}$ age constraints on the duration of resurgence at the Valles caldera, New Mexico: *Journal of Geophysical Research*, v. 112, B08201, 15 p. <https://doi.org/10.1029/2006JB004511>
- Randolph-Flagg, N., Breen, S., Hernandez, A., Manga, M., and Self, S., 2017, Evenly spaced columns in the Bishop Tuff (California, USA) as relicts of hydrothermal cooling: *Geology*, v. 45, p. 1015–1018. <https://doi.org/10.1130/G39256.1>
- Ross, C.S., and Smith, R.L., 1960, Ash-flow tuffs—Their origin, geologic relations, and identification: U.S. Geological Survey Professional Paper 366, 81 p. <https://doi.org/10.3133/pp366>
- Schmincke, H.-U., 2004, *Volcanism*: Berlin, Springer-Verlag, 324 p. <https://doi.org/10.1007/978-3-642-18952-4>
- Self, S., Heiken, G., Sykes, M.L., Wohletz, K., Fisher, R.V., and Dethier, D.P., 1996, Field excursions to the Jemez Mountains, New Mexico: New Mexico Bureau of Mines and Mineral Resources Bulletin 134, 73 p. <https://doi.org/10.58799/B-134>
- Sheridan, M.F., 1970, Fumarole mounds and ridges of the Bishop Tuff, California: *Geological Society of America Bulletin*, v. 81, p. 851–868. [https://doi.org/10.1130/0016-7606\(1970\)81\[851:FMAROT\]2.0.CO;2](https://doi.org/10.1130/0016-7606(1970)81[851:FMAROT]2.0.CO;2)
- Smith, G.A., and Lavine, A., 1996, What is the Cochiti Formation?: New Mexico Geological Society Guidebook 47, p. 219–224. <https://doi.org/10.56577/FFC-47.219>
- Smith, J.V., and Brown, W.L., 1988, *Feldspar Minerals, Volume 1—Crystal Structures, Physical, Chemical, and Microtextural Properties*: Berlin, Springer-Verlag, 828 p. <https://doi.org/10.1007/978-3-642-72594-4>
- Smith, R.L., and Bailey, R.A., 1966, The Bandelier Tuff—A study of ash-flow eruption cycles from zoned magma chambers: *Bulletin Volcanologique*, v. 29, p. 83–104.
- Smith, R.L., and Bailey, R.A., 1968, Resurgent cauldrons: *Geological Society of America Memoir* 116, p. 613–662. <https://doi.org/10.1130/MEM116-p613>
- Smith, R.L., and Dickson, K.O., 1965, Scapolite related to chlorine release in Bandelier Tuff, New Mexico: U.S. Geological Survey Professional Paper 525A, p. 149.
- Smith, R.L., Bailey, R.A., and Ross, C.S., 1970, Geologic map of the Jemez Mountains, New Mexico: U.S. Geological Survey Miscellaneous Investigations Map I-571, scale 1:125,000.
- Stimac, J.A., 1996, Hornblende dacite pumice in the Tshirege Member of the Bandelier Tuff—Implications for magma chamber and eruptive processes: New Mexico Geological Society Guidebook 47, p. 269–274. <https://doi.org/10.56577/FFC-47.269>
- Stimac, J.A., Broxton, D.E., Kluk, E.C., Chipera, S.J., and Budahn, J.R., 2002, Stratigraphy of the tuffs from Borehole 49-2-700-1 at Technical Area 49, Los Alamos National Laboratory, New Mexico (unpublished report): Los Alamos National Laboratory Report LA-13969-MS, 14 p.

- Stimac, J., Goff, F., and Goff, C.J., 2014, Intrusion-related geothermal systems, *in* Sigurdsson, H., Houghton, B., McNutt, S.R., Rymer, H., and Stix, J., eds., *The Encyclopedia of Volcanoes*, 2nd Edition: Amsterdam, Elsevier, p. 799–822.
- Sussman, A.J., Lewis, C.J., Mason, S.N., Geissman, J.W., Schultz-Fellenz, E., Oliva-Urcia, B., and Gardner, J., 2011, Paleomagnetism of the Quaternary Bandelier Tuff—Implications for the tectonic evolution of the Española Basin, Rio Grande rift: *Lithosphere*, v. 3, p. 328–345.
<https://doi.org/10.1130/L128.1>
- Utada, M., 2001, Zeolites in hydrothermally altered rocks, *in* Bish, D., and Ming, D., eds., *Natural Zeolites—Occurrence, Properties, Applications*: Mineralogical Society of America *Reviews in Mineralogy*, v. 45, p. 305–322.
- Utada, M., Shimizu, M., Ito, T., and Inoue, A., 1999, Alteration of caldera-forming rocks related to the Sanzugawa volcanotectonic depression, northeast Honshu, Japan—with special reference to ‘caldera-type zeolitization’: *Resource Geology Special Issue* 20, p. 129–140.
- Warshaw, C.M., and Smith, R.L., 1988, Pyroxenes and fayalites in the Bandelier Tuff, New Mexico—Temperatures and comparison with other rhyolites: *American Mineralogist*, v. 73, p. 1025–1037.
- Wright, J.V., 1981, The Rio Caliente ignimbrite—Analysis of a compound intraplinian ignimbrite from a major late Quaternary Mexican eruption: *Bulletin Volcanologique*, v. 44, p. 181–212.
- Zimmerer, M.J., Lafferty, J., and Coble, M.A., 2016, The eruptive and magmatic history of the youngest pulse of volcanism at the Valles caldera—Implications for successfully dating late Quaternary eruptions: *Journal of Volcanology and Geothermal Research*, v. 310, p. 50–57.
<https://doi.org/10.1016/j.jvolgeores.2015.11.021>